DESIGN AND CONSTRUCTION OF A MICROWAVE PLASMA ION SOURCE

A THESIS SUBMITTED TO
THE GRADUATE SCHOOL OF NATURAL AND APPLIED SCIENCES
OF
MIDDLE EAST TECHNICAL UNIVERSITY

BY

KAMİL ÇINAR

IN PARTIAL FULFILLMENT OF THE REQUIREMENTS
FOR
THE DEGREE OF MASTER OF SCIENCE
IN
PHYSICS

FEBRUARY 2011

Approval of the thesis:

DESIGN AND CONSTRUCTION OF A MICROWAVE PLASMA ION SOURCE

submitted by **KAMİL ÇINAR** in partial fulfillment of the requirements for the degree of
Master of Science in Physics Department, Middle East Technical University by,

Prof. Dr. Canan Özgen
Dean, Graduate School of **Natural and Applied Sciences** ⎯⎯⎯⎯⎯⎯

Prof. Dr. Sinan Bilikmen
Head of Department, **Physics** ⎯⎯⎯⎯⎯⎯

Prof. Dr. Sinan Bilikmen
Supervisor, **Physics Dept., METU** ⎯⎯⎯⎯⎯⎯

Examining Committee Members:

Assoc. Prof. Dr. Serhat Çakır
Physics Department, METU ⎯⎯⎯⎯⎯⎯

Prof. Dr. Sinan Bilikmen
Physics Department, METU ⎯⎯⎯⎯⎯⎯

Assoc. Prof. Dr. İsmail Rafatov
Physics Department, METU ⎯⎯⎯⎯⎯⎯

Dr. Burak Yedierler
Physics Department, METU ⎯⎯⎯⎯⎯⎯

Dr. Ali Alaçakır
Research and Development Department, SANAEM ⎯⎯⎯⎯⎯⎯

Date: ⎯⎯⎯⎯⎯⎯

I hereby declare that all information in this document has been obtained and presented in accordance with academic rules and ethical conduct. I also declare that, as required by these rules and conduct, I have fully cited and referenced all material and results that are not original to this work.

Name, Last Name: KAMİL ÇINAR

Signature   :

ABSTRACT

DESIGN AND CONSTRUCTION OF A MICROWAVE PLASMA ION SOURCE

Çınar, Kamil

M.Sc., Department of Physics

Supervisor   : Prof. Dr. Sinan Bilikmen

February 2011, 56 pages

This thesis is about the designing and constructing a microwave ion source. The ions are generated in a thermal and dense hydrogen plasma by microwave induction. The plasma is generated by using a microwave source with a frequency of 2.45 GHz and a power of 700 W. The generated microwave is pulsing with a frequency of 50 Hz. The designed and constructed microwave system generates hydrogen plasma in a pyrex plasma chamber. Moreover, an ion extraction unit is designed and constructed in order to extract the ions from the generated hydrogen plasma. The ion beam extraction is achieved and ion currents are measured. The plasma parameters are determined by a double Langmuir probe and the ion current is measured by a Faraday cup. The designed ion extraction unit is simulated by using the dimensions of the designed and constructed ion extraction unit in order to trace out the trajectories of the extracted ions.

Keywords: Ion Source, Microwave Plasma, Dense Plasma, Ion Generation, Ion Extraction

ÖZ

MİKRODALGA PLAZMA İYON KAYNAĞI TASARIMI VE ÜRETİMİ

Çınar, Kamil

Yüksek Lisans, Fizik Bölümü

Tez Yöneticisi   : Prof. Dr. Sinan Bilikmen

Şubat 2011, 56 sayfa

Bu tezin konusu mikrodalga iyon kaynağı tasarımı ve üretimidir. İyonlar, yoğun ve termal hidrojen plazması içinde üretilmiştir. Plazma, 2.45 GHz frekanslı ve 700 Watt çıkış gücünde mikrodalga kaynağı kullanılarak oluşturulmuştur. Üretilmiş mikrodalga kaynağı, 50 Hz'lik frekans atımlı mikrodalga oluşturmaktadır. Tasarlanan ve üretilen mikrodalga sistemi, payreks plazma kabı içinde hidrojen plazması üretmiştir. Ayrıca iyonları oluşturulan hidrojen plazmasından çıkarmak için iyon çıkarma ünitesi tasarlanıp üretilmiştir. İyon çıkarma başarılmıştır. Plazma parametreleri çift Langmuir sondası ile, iyon akımı ise Faraday kabı ile ölçülmüştür. Tasarlanan iyon çıkarma ünitesi boyutları kullanılarak iyon yörüngeleri simüle edilmiştir.

Anahtar Kelimeler: İyon Kaynakları, Mikrodalga Plazma, Yoğun Plazma, İyon Üretimi, İyon Çıkartımı

To my parents

ACKNOWLEDGMENTS

TABLE OF CONTENTS

LIST OF TABLES

TABLES

LIST OF FIGURES

FIGURES

CHAPTER 1

INTRODUCTION

Ion sources started to emerge while Goldstein was working on the canal rays in 1886 before designing low-current ion sources, which electron-atom collision mechanisms were used for [1]. In 1930's, by investigating the arc discharge, higher ion currents started to be provided. RF and microwave discharges started to be investigated during the next decadeand they were used in production of ion beams [1]. As it is seen that the origins of the ion sources are the atomic-nuclear physics research and ion implantation for microelectronic applications; moreover, ionization sources were developed for space propulsion applications in 1960's [2]. After all, ion sources have become indispansable parts of particle accelerators and ion implantation systems. For areas of usage, there are many types of ion sources with different working mechanisms; on the contrary, electron sources have limited variety [1, 2]. The ion types can be determined for the corresponding applications. Ion sources are mainly used to produce monoenergetic and unidirectional ion beams [2]. The generated beams are utilized by guiding them to ion beam lines or by direct guiding them to application zones.

There are plenty types of ion sources. The variety of the ion sources arises from the different ways of ion generation from solids, liquids and gases and also the variety of generating plasma such as DC discharge, arc discharge, RF discharge, microwave discharge and laser driven plasmas [2]. The general types of ion sources are listed in Table 1.1 and these ion sources can be divided into groups with respect to the ways of ion generation and areas of applications [1].

Table 1.1: Typical Ion Sources

Cathodes
Electron Bombardment Ion Sources
Plasmatron Ion Sources
Magnetron and Freeman Types Ion Sources
Penning Ion Sources
Multicusp Ion Sources
RF Ion Sources
Microwave Ion Sources
ECR Ion Sources
Laser Ion Sources
Electron Beam Ion Sources /Trap
Vacuum Arc Ion Sources
Large Area Ion Sources
Industrial Ion Sources
Liquid-Metal Ion Sources
Polarized Ion Sources
Cluster Ion Sources
Ion Diodes
Ion Sources for Space Applications

The ion sources or ion beam generators have a wide variety of units, such as plasma induction systems, ion extraction systems, electronic units that induce plasma and supply the extraction voltage. There are also units for guiding the ion beams. The ion sources necessitate an interacting multi-discipline study which should have the knowledge of plasma physics, electrical and electronics engineering, and computational systems.

In general, at the end of the ion beam line, there is a linear accelerator. The produced ion sources are connected to the open-end of this accelerator via vacuum cones. The accelerated ions are focused by an Einzel lens and dispersed by two quadrupole magnets. Moreover, a dipole magnet is used in order to deflect the accelerated ions, passing through the ion beam line. At the other end of the ion beam line, there is a target which is subjected to ion bombardment.

In this thesis, microwave ion sources have been investigated for the design and the construction. The designed and produced ion sources have been used for the ion beam lines.

In 1977, the first ion source was built by Sakudo and he also developed a microwave ion source with slit extraction [1]. Ishika, in 1984, used permanent magnets in order to built a compact

microwave ion source [1]. Afterwards the gradually increasing interest on microwave ion sources has spread over, because the microwave ion sources can reach high curret densities at low pressure plasmas.

The built-in microwave ion source system does not contain any magnetic confinement or any magnetic support for the plasma, like the electron cyclotron resonance (ECR) microwave discharges.

The organization of the thesis is as follows: In chapter 2, the theory of ion production via plasma is discussed and the mechanisms of the direct current (DC) plasma and the microwave (MW) plasma are reviewed. In chapter 3, the mechanism of the ion extraction is considered. In addition, the plasma (space) potential theory and the vacuum gradient are discussed. Characterization of ion beams and ion sources are explained in Chapter 4. The main part, the designed and constructed microwave plasma ion source is expressed in Chapter 5 where the produced parts of the system are explained. As the last chapter, Chapter 6, the data analysis of the ion source is done and the theoretical values of the designed system are compared with the simulation of the designed system and the measured data. Finally results and outcomes of the thesis are concluded.

CHAPTER 2

ION PRODUCTION VIA PLASMA

Altough there are many ways of producing ions, only ion production mechanism via plasma is the concern of this chapter. Ion production process can be divided into two parts. The first one is the production of raw ions from a generated plasma and the second is the extraction of the raw ions from the generated plasma.

2.1   PLASMA

In the universe, more than 99% of observed matter comprises plasma such as interstellar matter, nebulea, supernova, stars and also the flame [3]. Plasma is the fourth state of matter. If gases are heated, electrons of the gas molecules start to oscillate and the propability of ionization of the gas increases. In addition, electrons acquire more energy and their coupled atoms break up and move around freely. Consequently, the electrons prevail the electrostatic forces. If a quasineutral gas consists of charged and neutral particles which exhibits collective behaviour, this quasineutral gas is named plasma [4].

Quasineutrality is defined as approximately equal numbers of negative and positive charges existing in a system.

The collective behaviour of the plasma can be described by firstly comparing with the kinetic theory of gases. The kinetic theory of gases is that no net forces; such as, electromagnetic forces which act upon the gas particles. Because the gas particles carry no net charges, they are neutral. So the particles move in straight lines before they collide each other with a distribution of velocities (Gravitational forces are not our concern at this moment.) [5]. In plasma, charged particles create long range electromagnetic forces. Dominating motions

of the charged particles and local charge concentrations affect the whole plasma even if the local charge concentration is far from the concerning area. While the neutral particles exhibit straight line motions after their collisions with each other, the charged particles exhibit continuously changing motions because of electromagnetic forces between each other [5]. The electromagnetic forces are long-range forces and interactions which occur between the charged particles last. These continuous interactions of the charged particles do exhibit nonlinear behaviours. If there is a locally varied charges or a varied current distribution, there will be impacts on the whole plasma; i.e., the affected charged distribution will evolve into a new charged distribution.

In addition to the quasineutrality and collective behaviour of the plasma, the temperature, the number density of the particles and the most importantly, Debye length should be considered while defining the plasma.

Before defining the Debye length, the Debye shielding should be defined. The Debye shielding is the ability of the plasma to shield out electric potentials that are applied to the plasma [4]. The electric potentials can be produced by local charges or by inserting electrodes inside the plasma. The distance, where the potential vanishes, is called the Debye length. The Debye length, λ_D, is given by the expressions below [1].

$$\lambda_D^2 = \frac{\varepsilon_0 k T_e}{e^2 n_e} \quad , \tag{2.1}$$

$$\lambda_D = 743 \sqrt{\frac{T_e}{n_e}} \quad , \tag{2.2}$$

where k is the Boltzmann constant, ε_0 is the vacuum permittivity and e is the elemantary charge ($\sim 1.6 \times 10^{-19}$C (Coulombs)). The parameters, T_e and n_e are the electron temperature in electron volts, the electron number density in inverse cubic centimetre, respectively and the Debye length, λ_D is in centimeters [1]. If the Debye length λ_D increases, the density of the plasma will decrease; moreover, the Debye length, λ_D, increases with increasing kT_e. The unit of kT_e is Joule.

The Debye length also characterizes the plasma with additional parameters such as, N_D, which is the number of particles in the the Debye region [4]. N_D is computed by Equation 2.3 for a

Debye sphere which a sphere with a radius of λ_D.

$$N_D = \frac{4}{3} n_e \pi \lambda_D^3 \qquad (2.3)$$

The gas is considered as a plasma when the three conditions, below, are satisfied [4].

$$\lambda_D << L \quad , \qquad (2.4)$$

where L is the size of the plasma system. The dimensions of the plasma region should be much larger than the Debye length.

$$N_D >> 1 \qquad (2.5)$$

The number of particles should be much more than one in order to consider bulk of the charged particles as plasma.

$$\omega_p \tau > 1 \qquad (2.6)$$

Equation 2.5 is the requirement of the collective behaviour. In Equation 2.6, ω_p is the frequency of the plasma oscillations and τ is the mean time between the colllisions with neutral atoms. The plasma frequency should be more than the mean time of the collisions with the neutrals.

There are various ways to generate a plasma; however, two ways of generating plasma; such as DC (Direct Current) discharge, and MW (Microwave) discharge, have been mentioned respectively in this thesis. However, the microwave discharge have been discussed in detail.

2.2 DC DISCHARGE

A DC discharge can be achieved by applying a DC voltage between two conducting electrodes which are inserted into a gas at low pressures [5]. The typical gas pressure is in between 0.1 torr (0.133322 mbar) and 10 torr (13.3322 mbar) in order to process DC discharge plasma [3]. A schematic drawing of the set-up is given in Figure 2.1.
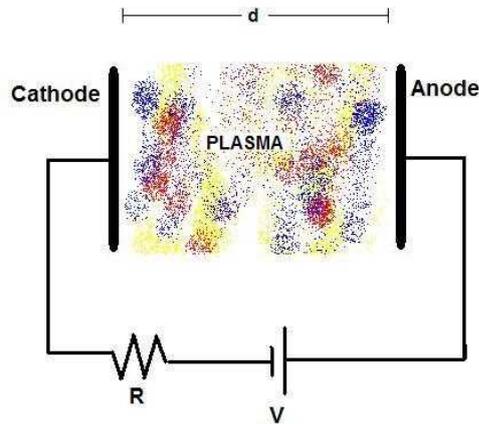
Figure 2.1: Schematic of a DC discharge

Any gas medium contains free ions and free electrons which arise from interactions between cosmic rays, environmental radiation with the gas atoms or a result of field emission from any violence on the surface, where electric fields are strong [3, 5]. These free charge carriers are accelerated through these electric field lines and they start to collide with the atoms or molecules, encountered with these free charge carriers [3].

These small amount of accelerated free charge carriers loses their kinetic energy by collisions; however, the voltage, applied to the electrodes, maintain these particles to build up their kinetic energies in order to ionize or excite targets that are the neutral particles, such as atoms and molecules [5]. If the kinetic energies of the free charge carriers are enough to exite or ionize the neutral particles, the accelerated charge carriers lose their kinetic energies by making inelastic collisions with the neutral atoms or molecules; otherwise, the collisions are elastic if the energy of the free charge carriers have too low to excite or ionize the targets which are the atoms and the molecules [5]. (Ionization is to break off electrones from the atoms whereas excitation is to bring electrons of an atom to a higher energy level than the electrons have.) With the ionization and excitation of the atoms or molecules, the number of produced charge cariers increases and an avalanche effect occurs. Besides of the free charge carriers, the produced ions and electrons contribute the excitation or ionization proccess in the medium. The produced ions and especially the produced electrons gain kinetic energy by the applied voltage. If there are elastic collisions between electrons and targets, the loss of the electron energy or the transfered energy can be calculated by Equation 2.7 [5]:

7

$$W_{tr} = \frac{2m_e}{M_T} W_e \quad , \tag{2.7}$$

where W_{tr} is the transfered energy to a target by an electron, M_T is the mass of the target, m_e is the mass of an electron and W_e is the energy of the electron. For the inelastic collions between the energetic electrons and the heavy target, the mechanism and the calculation of the collision change. The average fraction of the transfered energy is given by Equation 2.8 [5]:

$$\frac{W_{tr}}{W_e} = \frac{M_T}{m_e + M_T} \tag{2.8}$$

This avalanche effect is caused by the new produced electrons and ions. An electron multiplication process takes place. The number of electrons N, flowing through the anode electrode in a unit time, can be calculated by Equation 2.9 [3]

$$N = N_0 \frac{e^{\alpha d}}{1 - \gamma(e^{\alpha d} - 1)} \quad , \tag{2.9}$$

where N_0 is the initial number of electrons, α is the probability that the accelerated electron ionizes a gas atom as it travels a unit distance in the discharge tube (α is the first Townsend coefficient) [3, 6]. The term $e^{\alpha d}$ is the amplification factor at a distance of d. Beside of this, it is also the number of ions, produced by the primarily electrons. The coefficient γ is the efficiency of secondary electrons,e.i., the secondary electrons are produced by the ions, striking the cathode electrode. It is also called as the second Townsend coefficient [3, 6]. The secondary electron emission coefficient γ is determined by the type of metarial, which the cathode is made of, and the structure of the cathode surface; in addition to them, type of gas and reduced electric field E/p have importance [7]. Here, p is the pressure of the region where the plasma is formed.

The rapid transition, which is from a very poor electrical conductor with the resistivity of $\sim 10^{14} \Omega m$ to a relatively good conductor with a resistivity that is many orders of magnitude lower, characterizes the breakdown mechanism for the concerning gas, which is in a tube [3]. When the value of N goes to infinity, the electrical breakdown of the gas occurs in the gap between the two electrodes [3]. The electron amplification factor $\frac{N}{N_0}$, goes to infinity if the

denominator goes to zero in Equation 2.9. The condition of the electrical breakdown is given by Equation 2.10 [3].

$$\gamma(e^{\alpha d} - 1) = 1 \tag{2.10}$$

In order to sustain the DC plasma, the condition, below, should be provided [6].

$$\gamma e^{\alpha d} = 1 \tag{2.11}$$

In the case, $\gamma e^{\alpha d} \rightarrow 1$,the denominator of Equation 2.9 goes to zero and the number of electrons N goes to infinity. Because of the situation, the electric breakdown occurs.

In order to determine the value of α, α should be written in terms of parameters that change the value of α. An expression, designated as Equation 2.12, shows dependencies of α:

$$\alpha = Ape^{-Bp/E} \tag{2.12}$$

In Equation 2.12, the constants A and B differ for different gases and p is designating pressure of the gas. The term E determines the electric field of the interelectrode space and therefore $E = V/d$ [3]. The *breakdown voltage* or *starting voltage* V_{br} can be computed by combining Equation 2.12 and Equation 2.10 [3]. In addition to this, the breakdown is sustained at the room temperature 20^oC and the electron mobility is inversely proportional to pressure [7].

$$Apde^{-Bp/E} = \ln(1 + \gamma^{-1}) \tag{2.13}$$

By substituting the expression $E = V/d$ into Equation 2.13, the *breakdown voltage*, V_{br}, can be deduced as

$$V_{br} = \frac{Bpd}{\ln(pd) + \ln(A/\ln(1 + 1/\gamma))} \tag{2.14}$$

Expression 2.14, is known as *Paschen's Law* [3, 5, 6]. '*pd*' is called as the *reduced electrode distance*, on which the *breakdown voltage* depends. The graph of V_{br} versus *pd* is known as the *Paschen curve*. The value of *pd* plays important role in the extraction process of ions. The typical *Paschen curves* of several gases are given in Figure 2.2 [8].
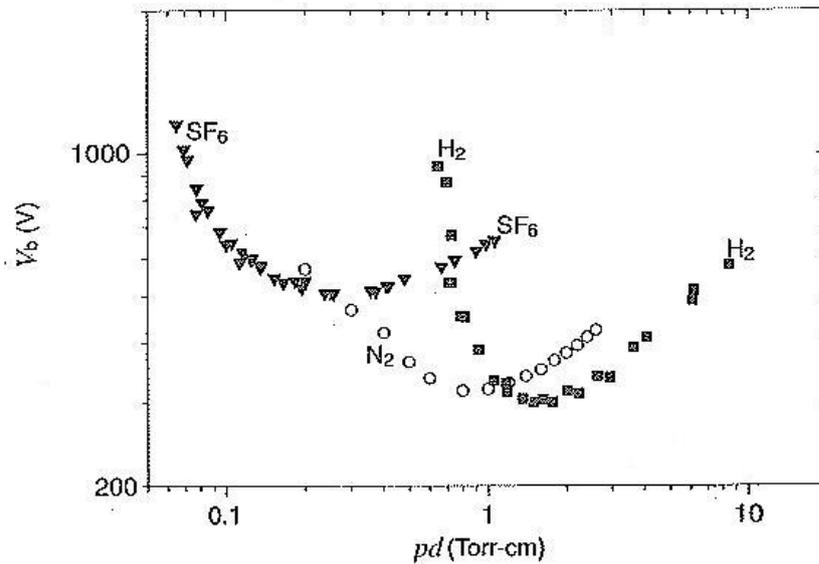
Figure 2.2: Paschen Curves at the temperature 20^oC [8](The graph is a log-log graph)

A typical voltage which is needed to sustain the discharge depends upon the type of gas and the pressure used in the plasma chamber [3]. And as it can be seen in Figure 2.2, the typical *breakdown voltage* is at the order of hundreds of volts. However, there is drastic increase at low pressures. Analysis for the low pressures gives the approximate values. The analysis is done numerically by using *GNU Octave*, which is a scientific computing software. The value of A and the value of $\ln(A/\ln(1+1/\gamma))$ are taken as 478.680 and 1.664 respectively. In order to compute the values of A and the value of $\ln(A/\ln(1+1/\gamma))$, the data points (2.06,1800.00) and (11.00,259.09) are taken from Figure 2.3 [9] and the estimated low pressure Paschen curve for the hydrogen gas is drawn as in Figure 2.4 . Note that the unit of *pd* is in cm-torr in Figure 2.4.

10
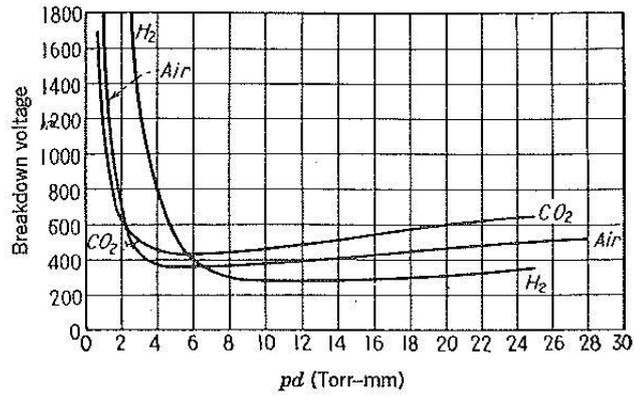
Figure 2.3: Paschen Curves at the temperature $20^{o}C$ [9]
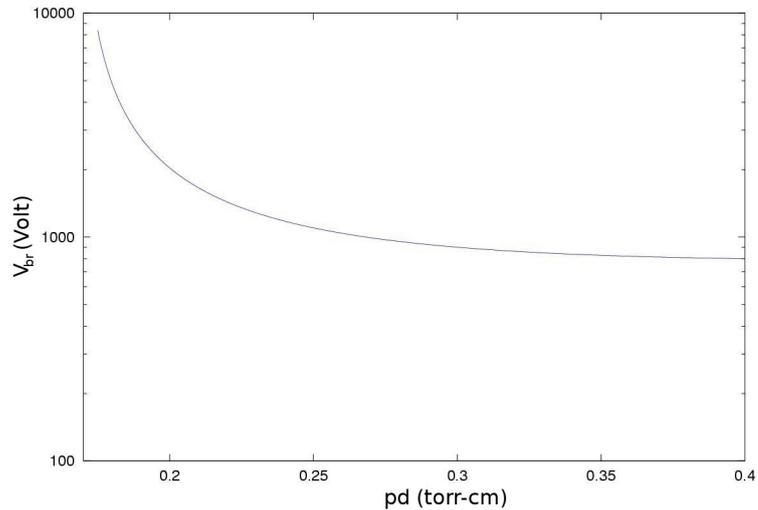
Figure 2.4: Estimated Paschen Curve for H_2. (This graph is a semilog graph.)

The breakdown voltage for the low values of *pd* is very important in order to prevent the breakdown at the extraction zone while applying high voltages. In addition to these, there is a crucial concept, *plasma potential* which should be explained distinctly in order to understand the ion extraction process.

DC discharge mechanism and DC discharge plasma ion sources are not the concern of this thesis directly; however, in an ion extraction process, a DC plasma can occur. To prevent the DC discharge at a vacuum gap, the mechanism of DC discharge should be well understood.

11

2.3 MICROWAVE DISCHARGE

The microwave generated plasmas have similarities with the RF (Radio Frequency) generated plasmas and optically generated plasmas. The wavelength of the microwaves are at the range of centimeters, longer than the optical waves which are with wavelengths in nanometer scale and smaller than the wavelength of RF radiation. Eventually, the all these radiation types are ordinary electromagnetic radiations, so the plasma generation could be described by the basic electromagnetic theory.

At first, the electric field of the microwave radiation can be considered in a rectangular waveguide. The microwaves can travel through any closed shaped metals. If these closed shaped metals are designed for the specific frequency, they guide electromagnetic waves, passing through them. For the frequency of 2.45 GHz, the rectangular waveguides are used and the mode of the microwave, which passes through them, is TE_{10} (Transverse Electric Field Mode 10, in rectancular waveguide). The mode of the wave determines the electric fields and magnetic fields of the wave across the width and the height of the waveguide [10]. The electric field distribution of the mode TE_{10} is depicted as in Figure 2.5. The electric field has a maximum in the center of the width of the waveguide [7]. The other modes can be used any microwave discharges but they are not the subject of this thesis.
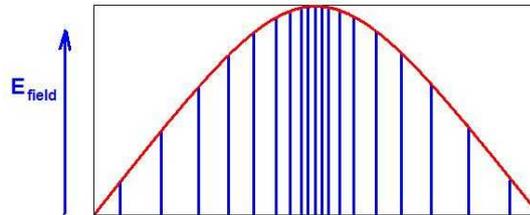
Figure 2.5: The TE_{10} mode of the microwave in a rectengular waveguide

The free electrons, which are produced by the background UV radiation or gamma radiations, are made to oscillate by the alternating electric field of the microwave. The TE_{10} mode is convenient for plasma generation in the rectangular waveguide becuase at the TE_{10} mode, the elecric field reaches its maximum value ath the midpoint of the waveguide [7]. When the free electrons start oscillating with the oscillating electric field, collisions with the neutral gas atoms become more violent, so these collisions heat up the gas. Due to the much larger

mobility of the electrons with respect to ions , the heating process is accepted to be sustained by the electrons. The heavier ions can not respond the rapid change in the electric field of the wave [5]. In this situation, the probability of ionization increases.
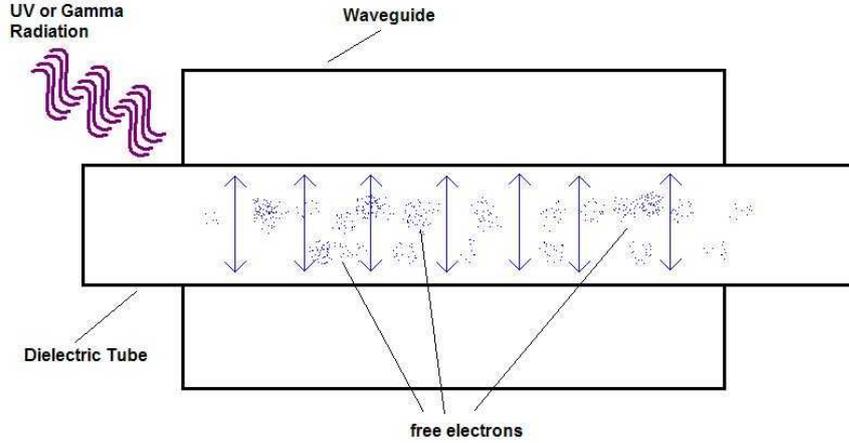
Figure 2.6: Ignition of a microwave plasma

The typical electric field strength of a 2.45 GHz microwave is approximately $E_0 \approx 30V/cm$ [5]. If the collisionless situation(i.e., the electrons do not collide with ions or neutrals) is considered, the equations of the motion of the electrons can be drived as follows:

$$\mathbf{E} = E_0 exp(-i\omega t)\hat{\mathbf{x}} \quad , \tag{2.15}$$

where E_0 is a constant with the same dimensions as $\mathbf{E}$.

$$\omega = 2\pi f \quad ,$$

where ω is the angular frequancy of the wave and f is the frquency of a microwave source. In this work $f = 2.45GHz$.

$$m_e \ddot{\mathbf{x}} = -e\mathbf{E} \quad , \tag{2.16}$$

where e is elementary positive charge,

$$\ddot{\mathbf{x}} = -\frac{e}{m_e}E_0 exp(-i\omega t)\hat{\mathbf{x}} \tag{2.17}$$

by integrating the previous equation, we can get the velocity of the electron,

$$\dot{\mathbf{x}} = -\frac{eE_0}{m_e}\left(\frac{1}{-i\omega}\right)exp(-i\omega t)\hat{\mathbf{x}} \qquad (2.18)$$

and by the second integration, we can get the position of the electron,

$$\mathbf{x} = \frac{eE_0}{m_e\omega^2}exp(-i\omega t)\hat{\mathbf{x}} \qquad (2.19)$$

The position of the electron is a function of time in Equation 2.19. The position can be rewritten as follows (Note that the following equation is a scalar function!).

$$x(t) = x_0exp(-i\omega t) \qquad (2.20)$$

The maximum distance x_0 that an electron is driven by the alternating electric field is given by

$$x_0 = \frac{eE_0}{m_e\omega^2} \qquad (2.21)$$

for the collisionless situation $v/\omega << 1$ should be provided where v is the elastic collision frequency in gases.

The kinetic energy of the oscillating electron, W_e, is written as

$$W_e = \frac{m_e v_e^2}{2} \qquad , \qquad (2.22)$$

where v_e is the speed of electron and it is the scalar quantity and the value of v_e is the magnitude of $\dot{\mathbf{x}}$. If the values of a radiation with a frequency of 2.45 GHz and a electric field strength of 30 V/cm are substituted into the above equations by converting them to SI units, the maximum distance that the electrons travel $x < 10^{-3}cm$ in a collisionless situation [5]. The maximum enegy that an electron gains in one cycle is about 0.03 eV [5]. This amount of energy is not enough to ionize the neutral atoms. So if the ignition is to be made at low pressures, there should be some manipulations done to the experiment to increase the probability of the ionization.

In collisional cases (the cases are at higher pressures than the first situations) it is to transfer the power from the outside electric field to the unit volume of gas and the average power $\bar{P}$ is given by [5]

$$\bar{P} = \frac{n_e e^2 E_0^2}{2m_e}\left(\frac{m_a}{v^2 + \omega^2}\right) \qquad , \qquad (2.23)$$

where m_a is the mass of the atoms that the electrons collide with. The elastic collision frequency , ν, is approximately in the order of between 10^9 and 10^{11} collisions per second at glow discharge conditions for gases [5].

The ionization of the neutral atoms becomes plausible in collisional situation. Random motions of electrons stem from the collisions with the atoms of the gas. Moreover, the electrons gain additional energy from the external electric field during each collision with the atoms. After an electron makes an elastic collision with an atom, it reverses its direction, at that instant of time, if the electric field changes direction, the electron accumulate enough energy to ionize the neutral atoms [5].

The plasma is ignited and maintained by the absorption of the electromagnetic energy and the heat exchange of the thermal plasma is provided by the convective cooling in the gas flow [7].

The incident electromagnetic radiation can only transfer a certain amount of its energy while travelling through the waveguide. The remaining energy is transmitted forward or reflected backward to the source by the thermal plasma. In order to increase the dissipated energy by the thermal plasma, the standing wave is formed by trapping the electromagnetic wave (i.e., the microwave.) [7]. As it is shown in Figure 2.7 and also in Figure 2.8, the standing wave pattern is formed through the waveguide. If special equipments like a stub tunner, a plunger, an isolater and a directional coupler, are used, the fraction of absorbed electromagnetic energy can be increased up to 90% to 95% [7].
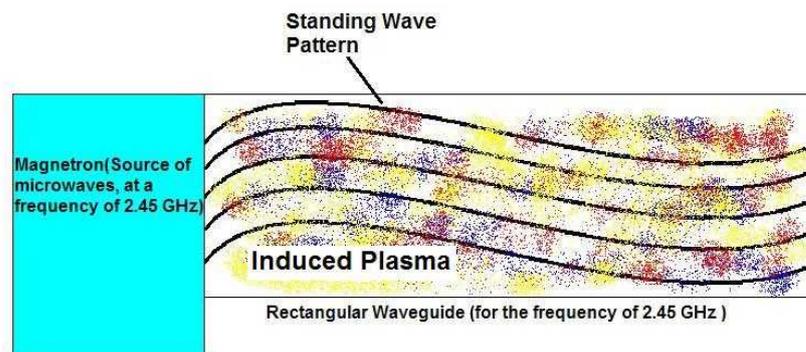

Figure 2.7: Standing wave pattern within the induced plasma

For the our designed system the location of the pyrex plasma discharge tube, which is almost

transparent for the microwaves (instead of the pyrex, quartz is usually used), crosses the waveguide horizontally.
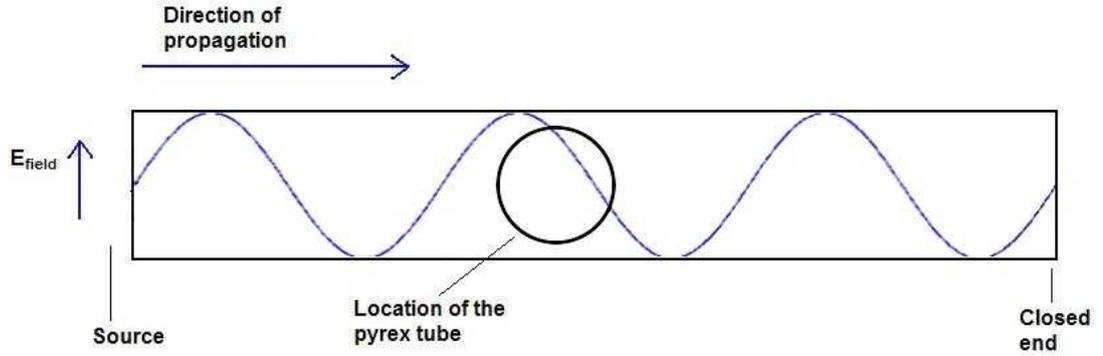
Figure 2.8: Location of the plasma tube across the standing wave

The microwave has a wavelength of 12.24 cm and the length of the waveguide is three times the wavelength of the corresponding microwave. There is a standing wave pattern of the system in Figure 2.8. The source of the microwave is on the left side of the waveguide and the right side of the waveguide is totally closed and sealed. The pyrex tube is intersecting the waveguide horizontally between the node and the antinode of the standing wave. At the left end of Figure 2.8, the oscillation of the electric field is shown. The oscillations of the electric field in the form of the standing wave induce a plasma inside the pyrex tube as shown.

Before, skipping to a new chapter, there is a very crucial remark that in the absence of magnetic confinement for the microwave discharge plasma. There is an upper limit for the electron number density (i.e., *number of electrons per cubic centimeter*), n_e, in the plasma [1].

$$n_e \leq 1.11 \times 10^{10} f^2 \quad , \tag{2.24}$$

where f is the frequency in GHz, and for the microwave with the frequency of 2.45 GHz the upper limit of the electron density is $n_e = 6.66 \times 10^{10} cm^{-3}$ [1]. The reason of existance of the upper limit is that the microwave will not be able to penetrate the plasma without applying a sufficiently high magnetic field (for f = 2.45 GHz, B = 0.0875 Tesla) through the plasma when the electron density reaches the upper limit. Moreover, the power of the microwave is absorbed at the surface of the plasma and the most of it reflects [1].

The details of the designed and built system are described in the following chapters with the help of the theoretical explanations, mentioned above.

CHAPTER 3

EXTRACTION OF IONS FROM PLASMA

The produced ions should be extracted from the plasma medium in order to direct them to targets or guide them to ion beam lines to distort profiles of ion beams. In order to collect the ions, a positive electrical potential is applied to the plasma medium with respect to the extracted zone and then ions are ready to be accelerated at the edge of the plasma medium. Accelerated ions are able to be guided and directed by the electric field and also a dipole magnet. In order to understand this procedure, *plasma (space) potential, extraction* should be discussed firstly. Also, the use of *vacuum apertures* will be explained for the production of *vacuum gradient*.

3.1 PLASMA (SPACE) POTENTIAL

For any practical plasma devices, plasma and walls of the plasma chamber produce a region, called sheath. Consider a plasma system which has no electric field inside or applied by any electrodes, inserted in. Since the electrons move much faster than the ions in the plasma, the electrons leave the plasma at a greater rate than the ions do [4, 7, 11]. The themal velocities of the individual particles can be calculated for the electrons and ions by using Equation 3.1 and 3.2 respectively.

$$v_e = \sqrt{\frac{3kT_e}{m_e}} \quad , \tag{3.1}$$

$$v_i = \sqrt{\frac{3kT_i}{M_i}} \quad , \tag{3.2}$$

where v_e is the speed of an electron and v_i is the speed of an ion. In Equation 3.2, the temperature of ions T_i and the mass of an ion M_i should be considered. The value of M_i/m_e is about 1837 for a hydrogen ion. From these equations, it can be deduced that the electrons' thermal velocities are about 1000 times faster than the ions' thermal velocities [7]. The fast moving electrons leave the plasma and stick to the walls of the chamber and the slow ions are assumed to be stationary with respect to the electrons, so that the plasma remains with a net positive charge [4, 7]. These excess charges produce a potential with respect to the walls. Debye shielding forms a potential variation in several Debye lengths. This layer is called *plasma sheath* [4, 11]. As F.F. Chen mentioned "The function of a sheath is to form a potential barier so that the more mobile species, usually electrons, is confined electrostatically. The height of the barrier adjust itself so that the flux of electrons that have enough energy to go over the barrier to the wall is just equal to the flux of ions reaching the wall [4]". The plasma potential drops while approching the wall. An illustration is shown in Figure 3.1.
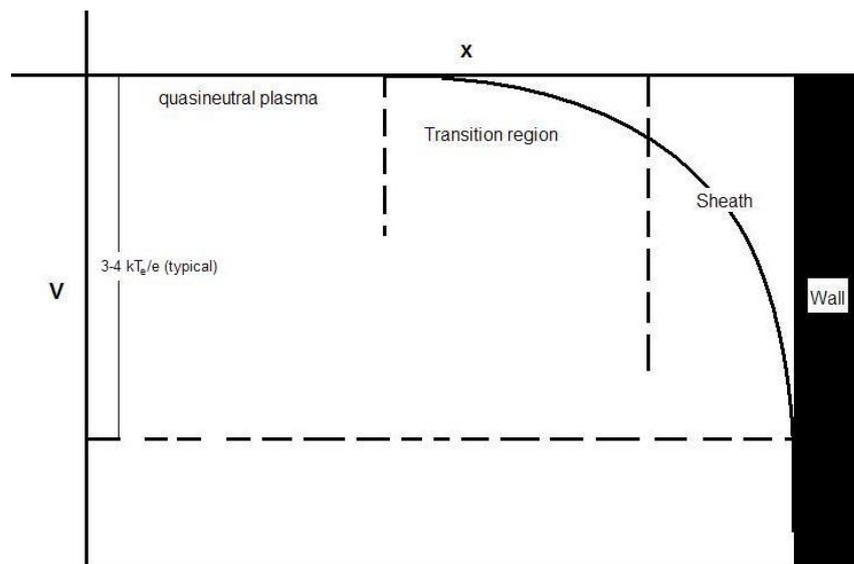
Figure 3.1: Plasma potential and the regions between the plasma and the wall

The reduction of the potential depends on the configuration and the plasma parameters yet it is typically 3 or 4 times the electron temperature (in electron volts) per charge of an electron (in Couloumb) and this situation is also valid for a floating probe or electrode which inserted in a plasma [11]. The floating electrode or probe can be said to be at the floating potential, negative with repect to the plasma potential.

In a situation that a conducting electrode immersed near the sheath and is held at a lower potential with respect to the plasma, the electrode attracts the ions and repels the electrons. If the electron density is taken to be zero at the sheath, the current density J can be written as [12]. Note that the charge state (or the ionization state) is taken as 1 for convenience while doing the drivations.

$$J = n_i e v_i \quad , \tag{3.3}$$

where n_i is the number density, e is the elementary charge in Coulombs and v_i is the speed of ions, respectively. The Possion equation is written for this region as

$$\frac{d^2 V}{dx^2} = \frac{n_i e}{\varepsilon_0} \tag{3.4}$$

By the conservation of energy (The calculations are non-relativistic calculations!),

$$M_i v_i^2 / 2 = eV \quad , \tag{3.5}$$

where M_i is the individual mass of the ions. The term $n_i e$ can be written in terms of J and v_i, then the Possion equation becomes

$$\frac{d^2 V}{dx^2} = \frac{1}{\varepsilon_0} \sqrt{\frac{M_i}{2e}} \sqrt{\frac{1}{V}} J(x) \tag{3.6}$$

If Equation 3.6 is multiplied by (dV/dx) and integrated from zero to a potential V [12, 13], we get

$$\left(\frac{dV}{dx}\right)^2 = \frac{4}{\varepsilon_0} \sqrt{\frac{M_i}{2e}} \sqrt{\frac{1}{V}} J(x) \tag{3.7}$$

By taking the square root of both sides of Equation 3.7, and then rearranging it,

$$\frac{dV}{V^{1/4}} = \frac{2}{\varepsilon_0} \sqrt{\frac{M_i}{2e}} J^{1/2}(x) dx \tag{3.8}$$

and then by integrating the above equation, the current density is found as

$$J(x) = \frac{4\varepsilon_0}{9} \sqrt{\frac{2e}{M_i}} \frac{V^{3/2}}{x^2} \tag{3.9}$$

Equation 3.9 is known as Child-Langmuir Law of space charge-limited current flow [4, 12, 13] and more general notation for ions having charge state (or ionization state) Z is [2]

$$J(x) = \frac{4\varepsilon_0}{9} \sqrt{\frac{2eZ}{M_i}} \frac{V_0^{3/2}}{x^2} \tag{3.10}$$

The Debye length is the crucial for the boundary of the plasma and for the dynamics of the transition region. For example, in the case of the high voltage applied to a electrode inside the plasma, the sheath region gets thicker than the Debye length and the sheath distance d_{sheath} can be written approximately as [11].

$$d_{sheath} \sim \lambda_D \sqrt{\frac{eV}{kT_e}} \tag{3.11}$$

Equation 3.11 becomes very important in order to detemine the probe sizes, dimension of wire meshes and the extraction apertures and separation [11].

3.2 EXTRACTION

The extraction process of ions from the generated plasma plays a crucial role while developing an ion source. Ions move randomly inside the plasma with free electrons. Each ion has a different kinetic energy. The ions should be made mono energetic and unidirectional before they are injected to a process chamber [2]. This is the reason why multi-farious electrodes are used. The general types of these are named as *accelerating grids or extractor grids or extractor mesh, (axial) diode system, triode diode extractor, mutigap extraction systems* and *multiaperture extractors* [1, 11]. All these types are basically simple particle accelerators with special geometrical design. The extractors should be designed while the limits of the Chid-Langmuir law is being taken into consideration.

Typical extraction techniques are shown in figures 3.2 , 3.3 , 3.4 [11]. In the present work, the technique shown in Figure 3.4 is modified. A basic extraction system can be designed as in Figure 3.2. For this design the target of the ion beams are not defined. For usual purposes, the

ions are driven to a vacuum chamber (or downstream region). This vacuum chamber can be held at a constant electrical potential. For the general case, if the electrical potential is applied to the vacuum chamber, where the ions
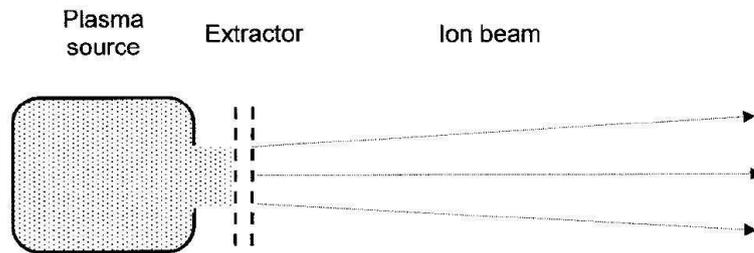
Figure 3.2: A basic extraction system with mesh extractors

impinge the corresponding target, the potential of the downstream region (vacuum chamber) should be taken into consideration. If the plasma is at the potential, V_{pl}, and the extractors' voltages are at the values, V_{ext1}, V_{ext2}, V_{ext3}..., and the potential of the vacuum chamber is at the potential, V_{ch}, then the general case of a extraction system can be thought as in Figure 3.3 with the given voltages.
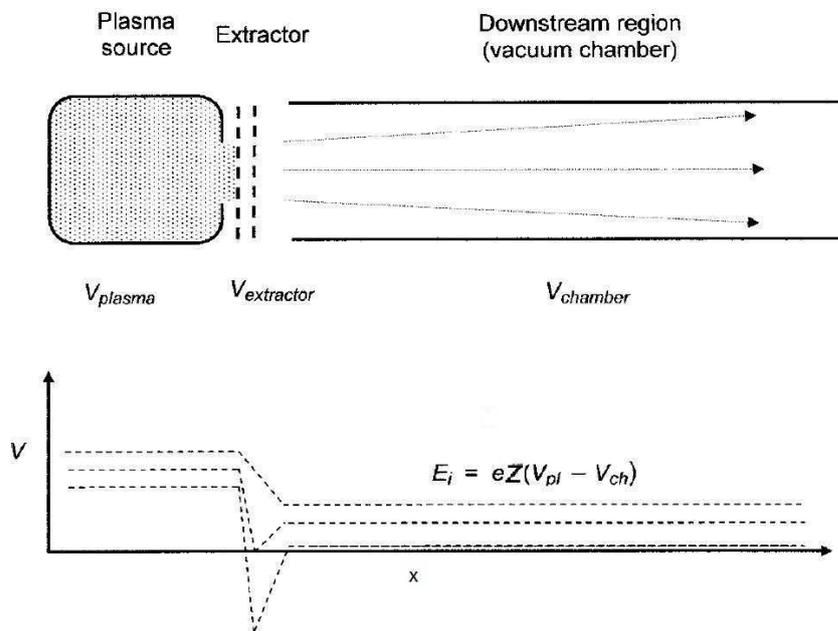
Figure 3.3: Extraction with the different extraction voltages

If the charge state Z of the ions are known, the energy of the ions, at the downstream region,

can be estimated as

$$E_i = eZ(V_{pl} - V_{ch}) \quad , \tag{3.12}$$

where e is the electron charge in units of Coloumb. Here the plasma potential is increased with respect to the chamber potential or any electrodes' potential by applying bias voltage to the plasma chamber. Nevertheless, the plasma voltage is higher than any potential, applied to the plasma chamber or any electrodes which are immersed in the plasma. The plasma potential is $3kT_e/e$ volts or $4kT_e/e$ volts higher than any high voltage electrode or frame, touching the plasma. It can be a good apprximation when the plasma potential, V_{pl}, is assumed to be equal to the potential of a extractor, V_{ext}, which are typically at the order of kilovolts [11]. For low energy ion sources and their applications, the plasma potential should be added to the voltage of the extractor and should be taken into consideration [11].

In this chapter, the axial diode extractor system, with a single axial aperture, is going to be discussed. For this type of extractor, a single aperture is used in order to let the ions go through it with the diameter, D, and the second aperture is located at a distance, d. Both apertures can have the same diameter. For the general case, the diameters of the two apertures are different as they are shown in Figure 3.4.
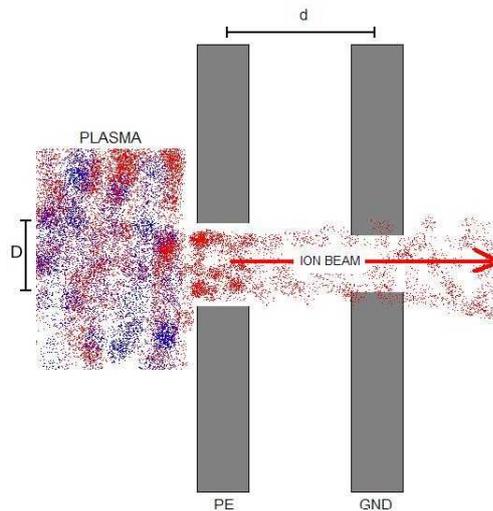

Figure 3.4: Extraction aperture diagram

For the designed system, the second aperture is narrower than the first single aperture, in

order to maintain the vacuum gradient between them. The vacuum gradient is discussed in the following section. It is worth to mention that the second aperture (at the second grounded electrode) determines the initial diameter of the ion beam. Plasma potential or the potential of the electrode, the neighbouring electrode of the plasma, is labeled as PE and the distant electrode is labeled as GND which means the *grounded electrode* in Figure 3.4.

This diode extractor is placed in front of the plasma source. It is important to be near the plasma. This extraction system is located as shown in Figure 3.5. The vacuum chamber is located after the diode extractor. A high voltage (about 3 kV) is applied to the first aperture electrode and the second aperture electrode and the vacuum chamber are grounded as they are shown in Figure 3.5. The potential of the plasma, V_{pl}, is assumed approximately equal to the potential of the first extractor, V_{ext1} ($V_{pl} = V_{ext1}$). Both the potential of the second extractor, V_{ext2}, and the potential of the vacuum chamber, V_{ch}, are grounded. Then the system becomes as it is shown in Figure 3.5. The energy of the beam ions is given by,

$$E_i = eZV_{ext1} \tag{3.13}$$
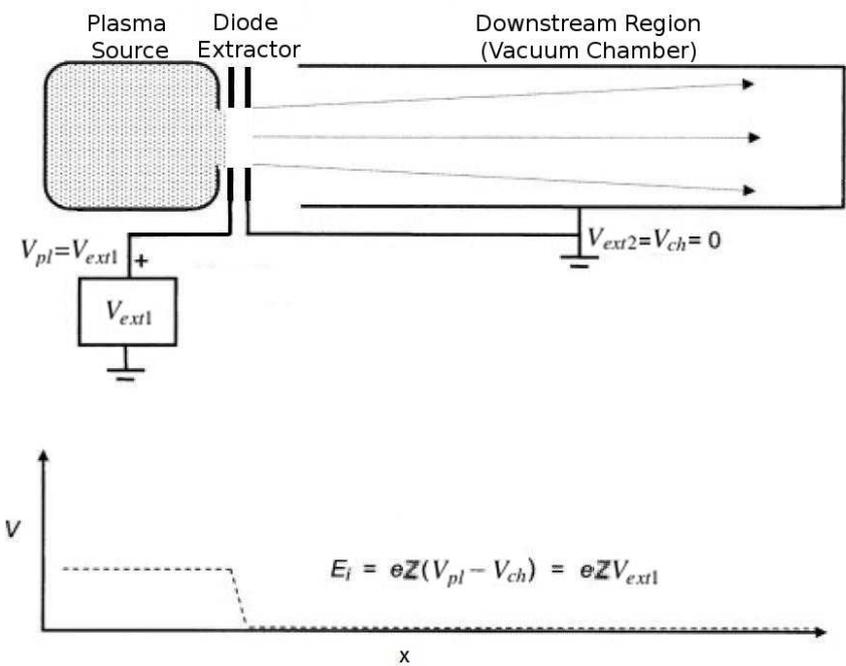
Figure 3.5: The extraction diagram for the designed system

Figure 3.5 is the schematic diagram of the designed system. For the rest of the thesis, discus-

24

sions would be based on this configuration. The importance of ion extraction will be discussed in Chapter 4.

3.3   VACUUM GRADIENT

Vacuum process is very impotant in this system. Unless the plasma is generated at a specific pressure, it will not be sustained and will not be stable. Moreover, the extraction process of the ions should be succeeded at very low presures in order to prevent the DC dischage between the extraction electrodes and the metal frames of the system.

In the designed system, the plasma chamber (tube) is held at a pressure of P_{plasma}. This pressure defines the plasma pressure. The place where the extraction electrodes are seperated, is held at a pressure of $P_{extraction}$ which is lower than the plasma pressure, P_{plasma}. Finally, the ion beam line or the measurement vacuum gradient part ends with a place which is held at the lowest pressure, named as $P_{beamline}$. The scheme is shown in Figure 3.6. The plasma pressure is controlled by the gas inlet which is located at the left side of the figure. The gap between the extraction electrodes is vacuumed by the rough vacuum. The rough vacuum of the whole system is also made from this connection as it is shown in Figure 3.6. The system is brought to the highest vacuum levels by the high vacuum pumps throught the turbo vacuum connection.
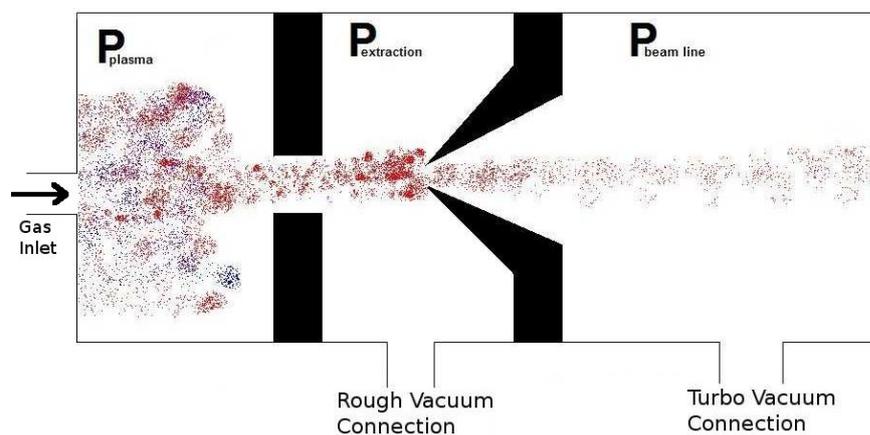
Figure 3.6: Vacuum zones in order to form the vacuum gradient

Finally, by applying the vacuuming process part by part, the vacuum gradient is sustained. To maintain the vacuum gradient, the separation of the apertures and the exraction aperture should be small enough and also the geometry of the apertures is very important. The conical separator is used to achieve the vacuum gradient in the system. In addition to these, the number of the vacuum separators between the vacuumed parts is also significant.

CHAPTER 4

CHARACTERIZATION OF ION BEAM AND ION SOURCE

4.1 PERVEANCE

Perveance defines the relation between the electron or ion beam current and the extraction voltage of the source with fixed cross-sectional beam area [2]. The perveance is given as

$$\mathcal{P} \equiv \frac{I_b}{V_0^{3/2}} = \frac{J\pi D^2}{4V_0^{3/2}} \tag{4.1}$$

In the above equation, I_b is the beam current and V_0 is the exraction voltage. D is defined as the initial beam diameter whereas J is the density of the beam current (look at Figure 3.4). For ideal ion sources, the extraction voltage would be applied via planar accelerating grids seperated by a distance d. The extraction voltage V_0 would operate with the accelareting grid with no webbing [2]. The ion current density can be written via the *Child space-charge limited condition*.

$$J = \frac{4\varepsilon_0}{9} \sqrt{\frac{2eZ}{M_i}} \frac{V_0^{3/2}}{d^2} \tag{4.2}$$

Here, Z indicates the charge state (or ionization state) of the ions. The Child-Langmuir law perfectly suits for estimating the maximum value of ion beam current [11]. More practical form of Equation 4.2 is given by [1]

$$J = (1.72) \sqrt{\frac{Z}{u}} \frac{V^{3/2}}{d^2} \tag{4.3}$$

where J is in units of miliamper per square centimeter (mA/cm^2), u is the atomic mass unit of the ions, V is in units of kilovolt (kV), and d is in the unit of milimeter (mm).

The ion beam current I_b, is determined by the smallest aperture of the extraction electrode and by multipying the current density J, with the area of the aperture, $\pi D^2/4$. The net current is found as

$$I_b = \frac{\pi D^2}{4} J \tag{4.4}$$

$$I_b = \frac{\varepsilon_0 \pi}{9} \sqrt{\frac{2eZ}{M_i}} \frac{V_0^{3/2} D^2}{d^2} \tag{4.5}$$

For an ideal ion source the perveance is found by substituting Equation 4.2 into Equation 4.1 as,

$$\mathcal{P}_{max} = \frac{J\pi D^2}{4V_0^{3/2}} = \frac{\pi \varepsilon_0}{9} \sqrt{\frac{2eZ}{M_i}} \left(\frac{D}{d}\right)^2 \tag{4.6}$$

It is better to design an ion source, having the value of the perveance which should be close the theoretical value of the perveance $\mathcal{P}_{max}$. In this work, the theoretical value of $\mathcal{P}_{max}$ is calculated as $2.53 \times 10^{-10}(A/V^{3/2})$ with respect to the dimensions of the designed extraction unit.

4.2 EFFICIENCY OF ION SOURCES

The power consumpsion of an ion source P_{is}, can be written by the sum of the power consumption of the extraction unit P_{eu}, and the power consumption of the plasma generator P_{pg}.

$$P_{is} = P_{eu} + P_{pg} \tag{4.7}$$

the power consumption of the extraction unit is given by [2],

$$P_{eu} = I_b V_0 \tag{4.8}$$

So Equation 4.7 becomes

$$P_{is} = I_b(V_0 + V') \quad , \tag{4.9}$$

where V' is the required potential (V) by the source to produce the ions and I_b is the ion current [2]. V' can be obtained by measuring the power consumption of an ion production unit which is used to produce raw ions for the system in order to obtain the ion current I_b. The power consumption of the ion production unit is calculated by $W_{ipu} = I_b V'$ for electrical devives. Where W_{ipu} is the dissipated power by the ion production unit for the corresponding ion current I_b. The electrical efficiency of the ion source, η_e, can be written as

$$\eta_e = \frac{P_{eu}}{P_{is}} = \frac{V_0}{V_0 + V'} \tag{4.10}$$

or alternatively,

$$\eta_e = \frac{1}{1 + (V'/V_0)} \tag{4.11}$$

4.3 REQUIRED GAS FLOW RATE

The imperative ingredient to provide the required plasma density is the gas . Firstly, the ratio of the ions' out flow from the source to the in-flow of the neutrals into the source determines the the gas utilization efficiency, η_g [2].

$$\eta_g = \frac{S_i}{S_n} = \frac{I_b}{eS_n} \quad , \tag{4.12}$$

where S_i and S_n are the out-flow and the in-flow rates, respectively. The term, S_n, is the flow rate of the neutrals into the plasma chamber.

The net efficiency of the ion source η_{is} is calculated by multiplying the gas utilization efficiency η_g, with the electrical efficiency η_e [2].

$$\eta_{is} = \eta_g \eta_e \tag{4.13}$$

If the in-flow rate of the gas is too low, it causes an extra load to the plasma generator and the efficiency decreases. The good utilization of the gas, for supplying the propellant to the ion source, is a very important effect on the ion sources.

4.4 ION FLUX AND NUMBER DESITY OF ION BEAM

In order to find out the number of the particles passing through a region per unit time, the ion flux should be considered. The ion flux, ϕ_i, of the system can be written by using the initial beam diameter, D [2].

$$\phi_i = \frac{J}{eZ} \tag{4.14}$$

and

$$J = \frac{4I_b}{\pi D^2} \tag{4.15}$$

by substituting Equation 4.15 into Equation 4.14

$$\phi_i = \frac{4I_b}{\pi eZD^2} \tag{4.16}$$

ϕ_i is in units of ions per square meter per second ($ions/m^2 s$). Moreover, the number density of the ion beam is calculated by using Equation 4.4 [2], and rewriting the equation for n_b which is the number denisty of the ion beam:

$$J = Zen_b v_b \quad , \tag{4.17}$$

$$n_b = \frac{J}{Zev_b} \tag{4.18}$$

or

$$n_b = \frac{\phi_i}{v_b} \quad , \tag{4.19}$$

where v_b is the mean velocity of the ions for the applied extraction voltage, V_0. From the conservation of energy (here the thermal energy of the ions are neglected) the mean velocity, v_b, is written as

$$v_b = \sqrt{\frac{M_i}{2eZV_0}} \tag{4.20}$$

If equations 4.2 and 4.20 are substituted into Equation 4.18, the number denisty of the ion beam, n_b, is found as

$$n_b = \frac{4\varepsilon_0 V_0}{9eZd^2} \tag{4.21}$$

As it can be seen explicitly in Equation 4.21, the ion density is independent of the ion mass and the unit of the number density is in ions per square meter ($ions/m^2$).

CHAPTER 5

THE DESIGNED SYSTEM

A microwave coupled plasma ion source is designed and constructed in this work. The microwave generation is provided by a magnetron which has the output power of 700 Watt with the frequency of 2.45 GHz. Since the high voltage power supply of the magnetron alternates with the frequency of 50 Hz, the generated microwaves pulse with the frequency of 50 Hz. The power supply of the magnetron has a half-wave rectifier, so the magnetron also turns off after each cycle of the alternating current. When the magnetron is turned on, the microwave generation starts with the maximum power. The magnetron is cooled by air ventilation. The *3D design* of the microwave generator is shown in Figure 5.1.
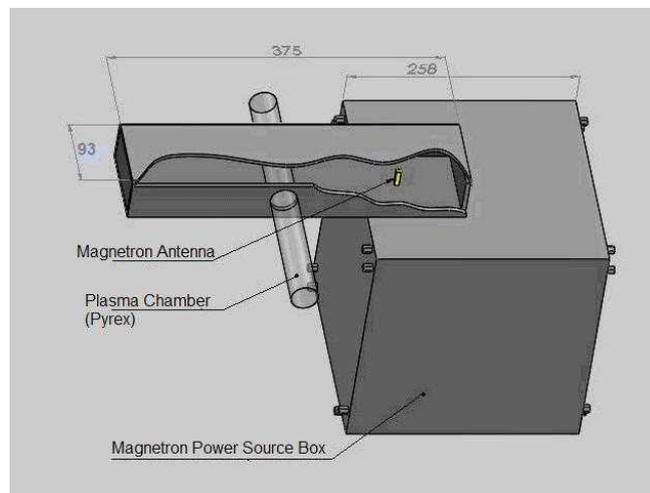

Figure 5.1: Microwave generator with the integrated power source, the waveguide and a pyrex plasma chamber

The dimensions of the waveguide are determined with respect to electromagnetic waves with the frequency of 2.45GHz which sits in the microwave region of the electromagnetic spec-

trum. The inside height of waveguide is 45 mm whereas the inside width is 93 mm. Because of the type of the rectangular waveguide, the mode of the propagating wave is TE_{10} inside the waveguide.

As they are shown in Figure 5.2, all the parts of the system numbered and titles of the numbered parts are given in Table 5.1.
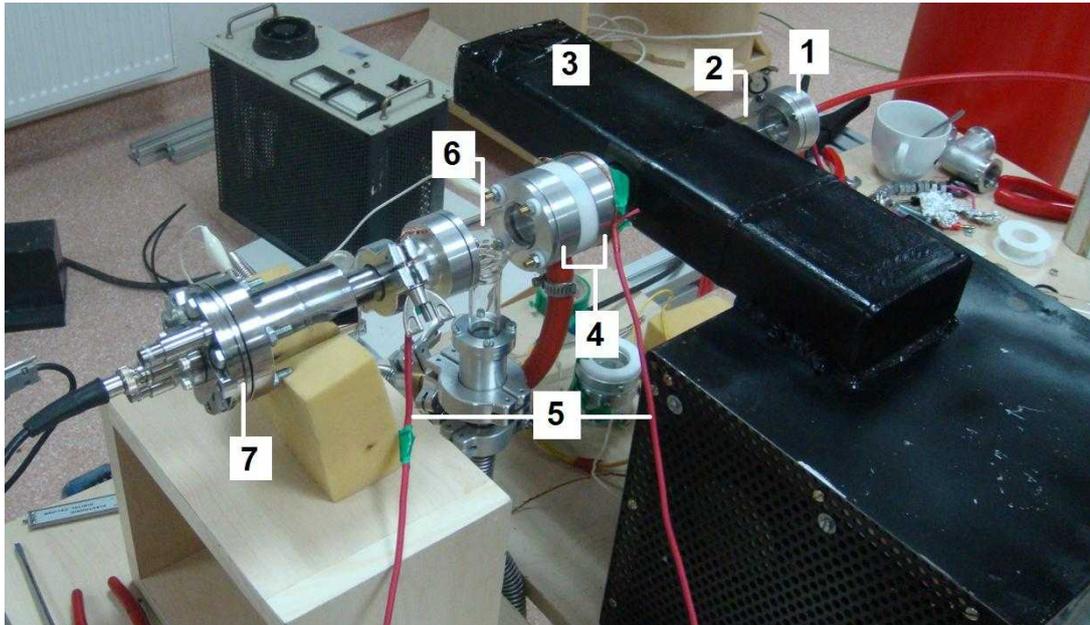
Figure 5.2: Microwave generator with the integrated power source and the general view of the assembled system

Table 5.1: Parts and components of the system

1	Gas Inlet
2	Plasma Chamber (Pyrex Tube)
3	Waveguide
4	Extraction Electrodes
5	High Voltage Cables
6	Vacuum Gradient
7	Faraday Cup

In Figure 5.3, the system is unmounted from the waveguide and the parts are named as in Table 5.2.

33
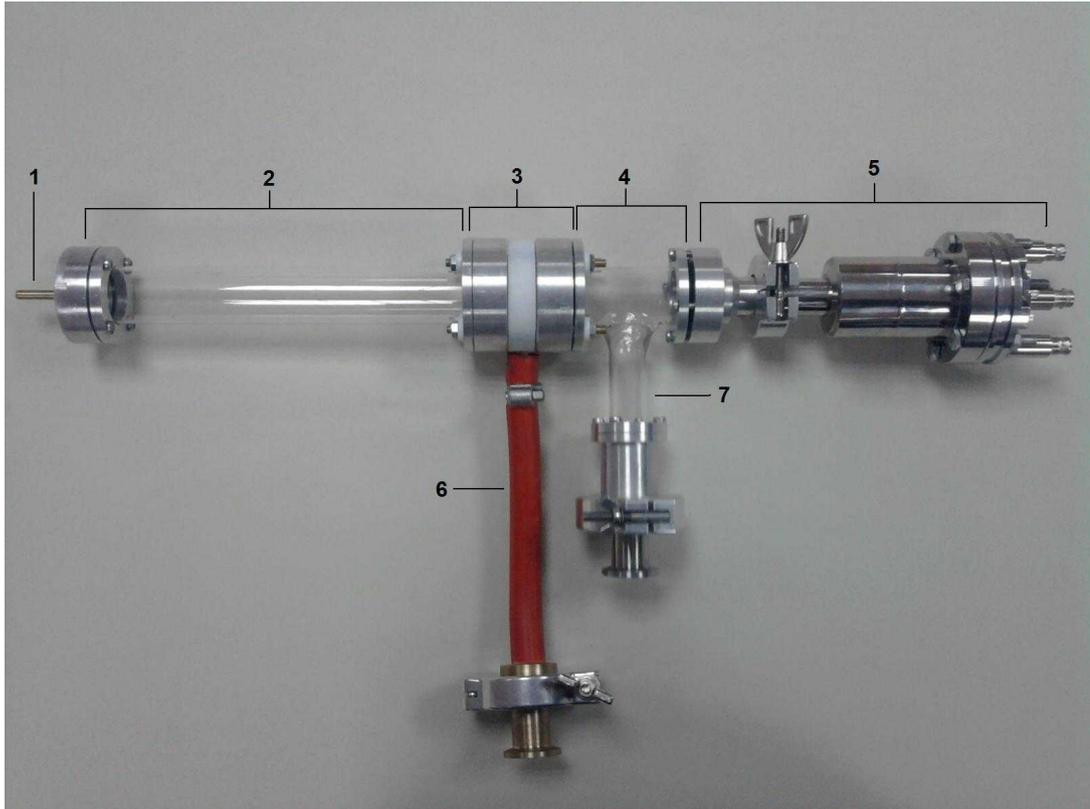
Figure 5.3: Assembled system without the microwave source

Table 5.2: Names of the parts in Figure 5.3

1	Gas Inlet
2	Plasma Chamber (Pyrex Tube)
3	Extraction Unit
4	Vacuum Gradient
5	Faraday Cup Unit
6	Vacuum Line (for the extraction unit)
7	Vacuum Line (for vacuum gradient)

5.1   PLASMA GENERATION BY MICROWAVES

The microwave ion generation unit of the system comprises of a waveguide with the length of 375 mm and a pyrex plasma chamber, mounted through the waveguide horizontally. The circular holes that hold the plasma tube have a diameter of 30 mm in order to mount the pyrex plasma chamber tightly.
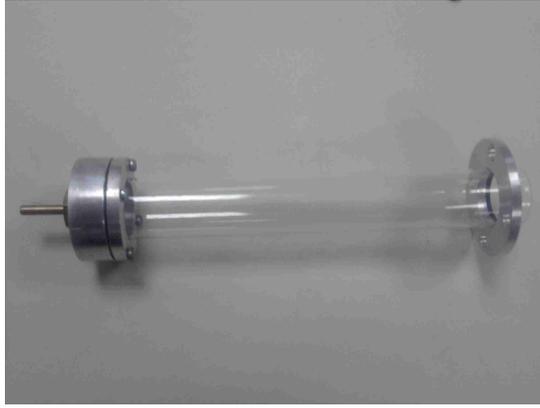
Figure 5.4: The Pyrex Plasma Chamber; with the gas inlet connector on the left side

The ends of the waveguide are closed and sealed in order not only to produce standing wave pattern inside the waveguide, but also to prevent microwave leakage. The generated microwaves are pumped in near the end of the waveguide via the microwave antenna of the magnetron. The length of the waveguide is approximately 3 times longer than the wavelength of 2.45 GHz microwave. The plasma is generated between the nodes of the standing waves. In Figure 5.5, the photograph of the microwave induced plasma system is shown while the microwave induced plasma is forming through the pyrex plasma tube.
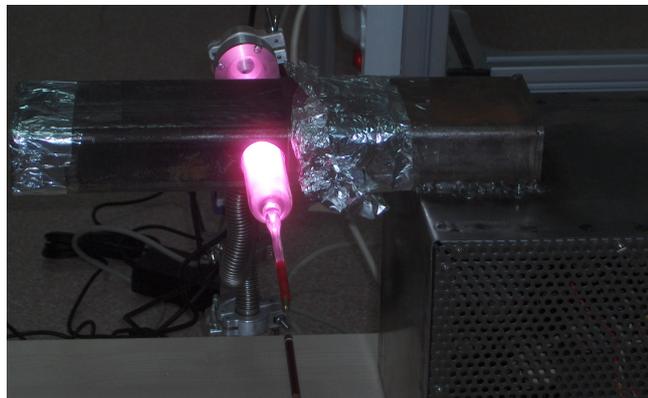
Figure 5.5: Plasma generation in oder to test the microwave unit

The plasma characterization is done by using a double Langmuir probe. The data of the current is measured by Keithley-2400 Sourcemeter and is collected by Labview-9 via GPIB (General Purpose Interface Bus) interface. The double Langmuir probe is inserted into the plasma at a horizontal position through the cylinderical symmetry axis of the pyrex chamber

in order to find out the plasma parameters, such as the electron density, n_e, and the electron temperature, T_e. The data sets are taken at the dispersion zone of the plasma. The dispersion zone is shown in Figure 5.6, where the plasma disperses to the ends of the chamber when it pervades from borders where the waveguide encompasses the chamber.

Figure 5.6: Dispersion zone

In order to measure the plasma parameters, the double Langmuir probe, used in this system, is shown in Figure 5.7. The double Langmuir probe was prepared especially for this system. The probe has a pyrex probe tube, prepared as the body (1) of the probe. The ends of the body are sealed. Two copper wire lines (2) cross through the pyrex body and are connected the tungten wire lines which end at the tips of the probe. The connection part (3) is made of aluminium and it connects the probe to the plasma chamber (tube). There is a O-ring, got clamped inside the connection part. This clamped O-ring allows to adjust the location of the probe tips in the plasma chamber by moving through the axis of the body (1) and also prevents gas leakage inbetween the body(1) and the connection part (3). The tips (4) are made of tungsten.
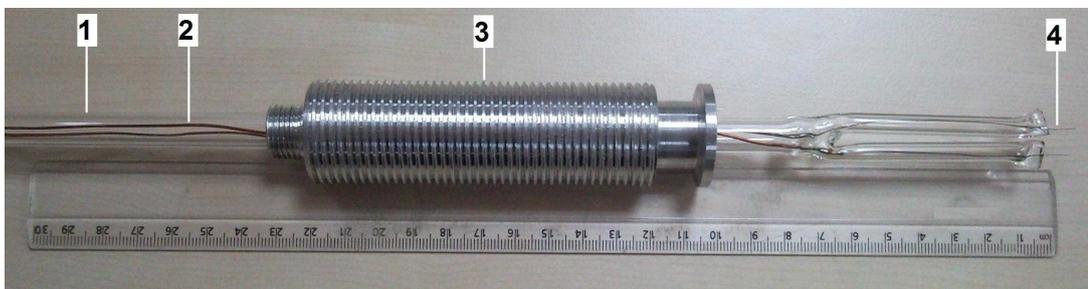

Figure 5.7: The double Langmuir probe

There is a closer view of the double Langmuir probe in Figure 5.8. The two tips are separated from each other by two pyrex tube branches and the tungten wires are soldered to the copper wires at the joining point of the two branches. The length of these branches are 6.5 cm long approximately. The diameter of the each probe tip is 0.25 mm and the length of the tips is 10 mm. The total surface area of the each pobe is $7.9 mm^2$.

After the tips of the probe are immersed into the plasma, a voltage source is connected to the electrodes of the tips. The voltage is increased gradually from -70V to +70V. The current and the voltage difference between the two tips are measured and saved at the computer.

Figure 5.8: The tips of the probe

The tips of the probe are localized at 50 mm away from the center of the waveguide's symmetry axis. The localization of the tips of the probe are shown in Figure 5.9(a) and in Figure 5.9(b). In Figure 5.9(c), the double Langmuir probe is mounted and operated and it can been seen as a silver color cylinderical metal on the right-hand side of the plasma chamber. In order to prevent the noise stemming from the microwave with the frequency of 2.45 GHz, the tips of the probe are located out side of the waveguide. If the data are taken at the position mentioned above, the comparison can be made consistently while the plasma parameters are investigated at the midpoint of the waveguide. Moreover, a filtration process is applied while the plasma is forming. Low pass filter is used at the frequency of 0.1 Hz.

The values of the electron number density n_e and the electron temperature, T_e at the midpoint of the waveguide are expected to be more than the values, measured at the dispersion zone, which is the outside of the waveguide.

(a) The plasma is off
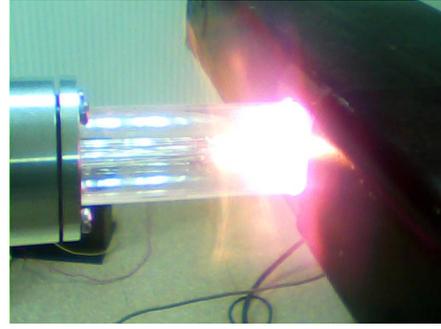
(b) The plasma is on
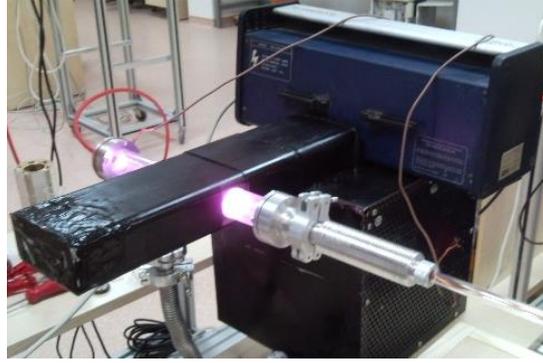
(c) whole view

Figure 5.9: The location of the probe tips

The current versus voltage graph of the microwave induced plasma, at the pressure of 1.5 mbar (1.13 torr), is shown in Figure 5.10. The plasma electron temperature, T_e, and the electron denisty, n_e, are calculated by using the following equations [14]:

$$\left.\frac{dI_{prob}}{dV_{prob}}\right|_{I_{prob}=0} = \frac{1}{2}\frac{eI_+}{kT_e} \quad , \tag{5.1}$$

$$T_e = \frac{1}{2}\frac{e}{k}\Delta V_d \quad , \tag{5.2}$$

where A is the area of the individual tip surface, V_{prob} is the voltage difference between the tips of the double probe, I_{prob} is the probe current, I_+ is the saturation current, k is the Boltzmann constant, and m_+ is the mass of the hydrogen ion H^+.

38
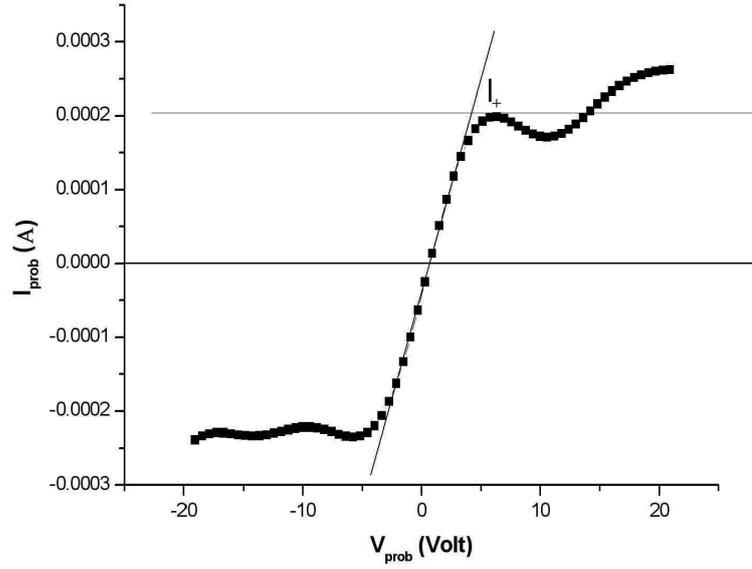
Figure 5.10: The Current vs Voltage Graph of *1,5 mbar Microwave Hydrogen Plasma at the dispersion zone 1*

By using the graph, above, the probe current I_{prob} is obtained as $\sim 250\mu A$ and the ion saturation current, I_+, is determined as $\sim 200\mu A$. In order to determine the slope of the linear part of the curve at $I_{prob} = 0$, the value of the probe current, at $250\mu A$, and the value of the probe voltage, V_{prob}, at $4.38V$ can be used. By substituting the values of the probe current $I_{prob} =\sim 250\mu A$ and the corresponding voltage, $V_{prob} = 4.38V$, into Equation 5.1, the expression can be written as

$$\frac{250 \times 10^{-6}}{4.38} = \frac{1}{2}\frac{e}{kT_e} \times 200 \times 10^{-6} \tag{5.3}$$

If the above equation is arranged for T_e, then T_e is found approximately $\sim 2eV$ ($\sim 23200^o K$).

$$n_e = \frac{I_+}{0.61eA \sqrt{kT_e/m_+}} \tag{5.4}$$

The ion saturation current, I_+, can be determined by drawing a tangential line horizontally to the first crest of the ion current decline at the positive voltage region. This is done for fitting and determining the tangent hyperbolic characteristic of the double probe's *I vs V curve*. It should not be forgotten that this procedure is approximate determination of the ion saturation

39

current. If the ion saturation current, I_+, is $\sim 200\mu A$ is substituted into Equation 5.4 [14], Equation 5.4 becomes

$$n_e = \frac{200 \times 10^{-6}}{0.61 \times 1.6 \times 10^{-19} \times 7.9 \times 10^{-6} \sqrt{1.38 \times 10^{-23} \times 23200/1.6 \times 10^{-27}}} \tag{5.5}$$

Finally, the electron density, n_e, is calculated for the pressure of 1.5 mbar to be $2 \times 10^{16} m^{-3}$ or $2 \times 10^{10} cm^{-3}$.

By repeating the experiment, the following data were taken and the graph is shown in Figure 5.11, in order to obtain the plasma electron temperature and density at the midpoint of the waveguide. The pressure was held at 1.5 mbar and again the hydrogen gas was used. By using the graph, in Figure 5.11, and by doing the same calculations, mentioned previously, the electron temperature, T_e, is obtained as $\sim 8eV$ ($\sim 92800^o K$), and the electron denisty, n_e, is obtained in the order of $\sim 7.5 \times 10^8 cm^{-3}$. As it can be seen from the value of the electron number density, n_e, it is smaller than the value which is found for the data of the dispersion zone, is in the order of $10^{10} cm^{-3}$.
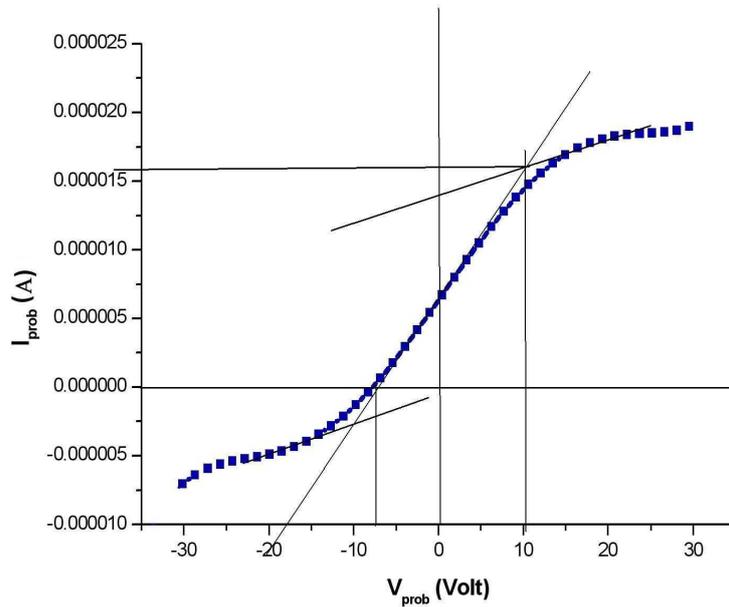

Figure 5.11: The Current vs Voltage Graph of *1.5 mbar Microwave Hydrogen Plasma at the midpoint of the waveguide*

As it is seen in Figure 5.11, the *I vs V curve* of the probes is not symmetric about the origin.

And also the found ion density is smaller then the *dispersion zone 1*. It is not an expected value for the core of the plasma.

The experiment was repeated again in order to obtain the symmetric *I vs V curve* of the plasma outside of the waveguide. The probe tips were at a distant of 57 mm from the midpoint of the waveguide. The reason of this is to observe the electron density decrease while moving the probe to the outside of the waveguide. The data were taken for the microwave hydrogen plasma at the pressure of 1.5 mbar. The graph of this process is shown in Figure 5.12.
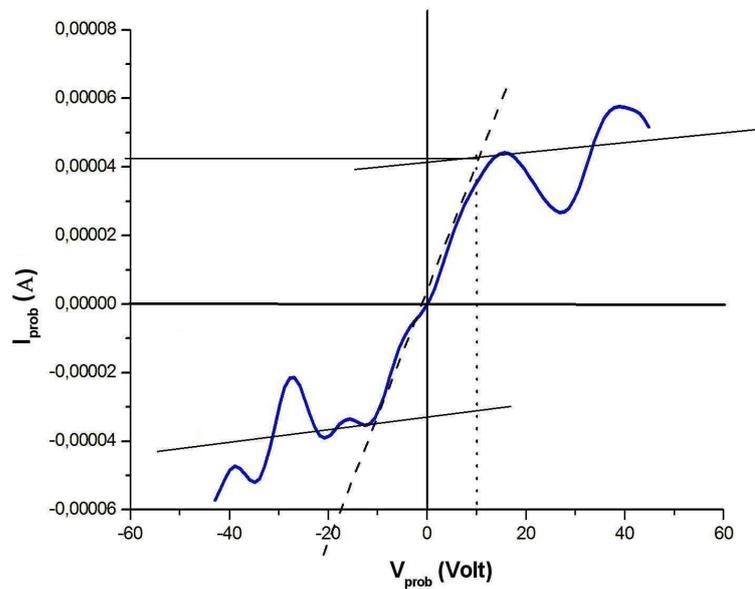
Figure 5.12: The Current vs Voltage Graph of *1.5 mbar Microwave Hydrogen Plasma at the dispersion zone 2*

If the data analysis above is applied, the electron temperature, T_e, is obtained as $\sim 5eV$ ($\sim 58000^o K$), and the electron denisty, n_e, is obtained in the order of $\sim 10^9 cm^{-3}$ at the distant, 57mm far from the midpoint of the waveguide and in the vicinity of the extraction electrodes.

As it can be seen from the result of the calculation, the electron density of the plasma decreases when the plasma disperses. However, the second *I vs V Graph* in Figure 5.11 is not as accurate as the first *I vs V Graph*, in Figure 5.10. The reason of this is that the second *I vs V Graph* is not symmetric with recpect to the origin and there is a shift on the graph. While the data are been taken out side of the waveguide, at *the dispersion zone 2*, the plasma can be affected by

the environmental impacts. And also at a little far distant, out of the waveguide, the plasma becomes more instable. Since the microwaves can not provide the sufficient energy to the molucules in order to ionize them at that region. The plasma starts flickering far from the waveguides borders. The waved shapes, at the left and right sides of the curve, can be caused by these instabilies at *the dispersion zone 2*. The region, where the data are taken accurately is very narrow in this experiment. However, there is some noise, observed in the waveguide that is not eliminated. Consequently, for the data of the dispersion zones, the current readings and the voltage readings are more accurate than the data of the midpoint zone. While taking the data sets of the experiment, the noise factors are discarded by low pass filters via the computer. The filter tools are used to get rid of the noise factors in the computer programme. However, these filtering tools are not electronic tools, they are only the computational tools that reduce some of the unwanted signal while the *I vs V Graphes* are being drawn and they are not enough to get rid of the noise and the other effects which occured at the midpoint of the waveguide. The other effects are discussed at the conclusion part of the thesis. While doing the experiment, the data, which were obtained for the 1.5 mbar microwave plasma at the dispersion zones, have been used in the calculations and comments.

5.2 EXTRACTION UNIT

In this experiment, the diode extraction system is used with the single aperture. There is a disassembled view of the extraction unit in Figure 5.13 and the parts are named as in Table 5.3.
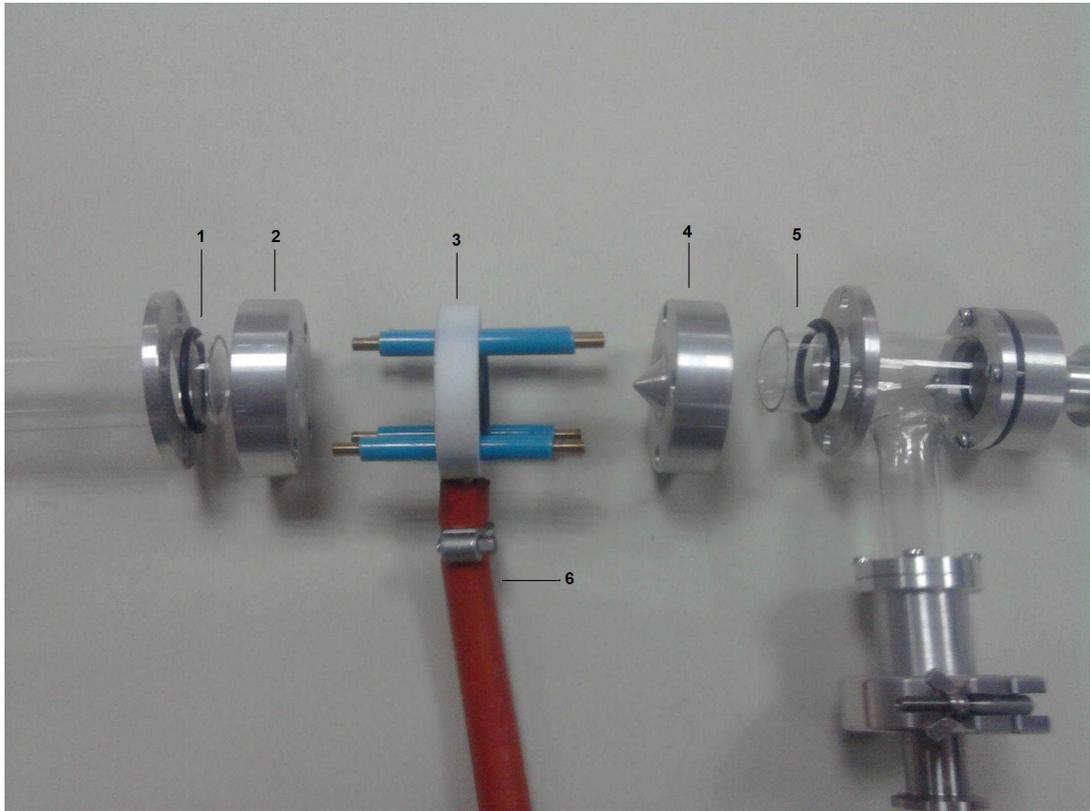

Figure 5.13: Dissembly of the extraction unit

Table 5.3: Explanation of Figure 5.13

1	Plasma Chamber Connection
2	First Single Aperture
3	Teflon Separator
4	Conical Single Aperture
5	Vacuum Gradient Connection
6	Vacuum Line

The plasma chamber connection is made of aluminium in the shape of a disk which joins the

first single aperture with four bolts and an O-ring is placed inbetween the plasma chamber connection and the first single aperture. All the o-rings are lubricated with low pressure lubricant.

In Figure 5.14(a), the plasma side of the first single aperture is shown. This side faces the plasma chamber and the plasma chamber is mounted in this side. In Figure 5.14(b), the teflon separator side is shown. This side faces the teflon separator and presses the teflon separator with four long bolts which connect the first single aperture, the teflon separator and the conical single aperture together. The side, facing the teflon separator, is smooth and flat to provide a proper vacuum. The diameter of the aperture is 4 mm and the thickness of the aperture has a width of 1 mm, approximately.

(a) Plasma Side   (b) Teflon Separator Side
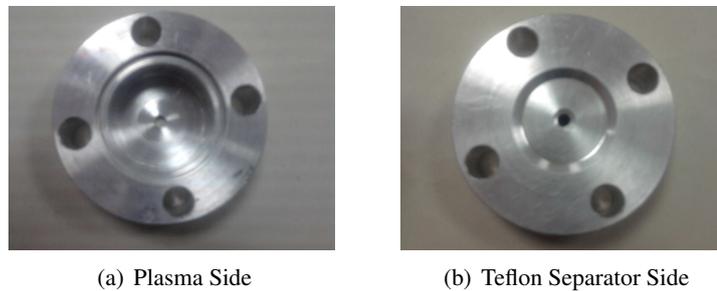
Figure 5.14: The First Single Aperture

The conical single aperture is shown in Figure 5.15. The conical side faces the teflon separator and it has an aperture, with the diameter of 2 mm, at the tip. The reason of the conical shape is to produce curved electric field lines in order to guide the accelerated ions to the aperture. In Figure 5.15(b), the teflon separator side of the conical aperture is shown. This side has a smooth and flat surface, like the teflon separator side of the first single aperture, in order to make perfect contact with the teflon separator. The other side of the conical single aperture has a cavity (in Figure 5.15(c)), like the first single aperture has also, in order to join the vacuum gradient part. And this side is mounted to the vacuum gradient part with an O-ring and a aluminium connection disk. Both the first single aperture and the conical single aperture are used as the electrodes in order to apply the extraction voltage.

In Figure 5.16, one side of the teflon separator is shown. The teflon separator is used for an isolator in between the two extraction electrodes, which are also the apertures of the exraction unit. Besides of being used as an isolator, it is very durable for the vacuum and is convenient to

44

be processed and shaped. The teflon separator has O-rings and cavities on its both sides. The O-rings are placed in the coves and they make perfect connections with the first single aperture and the conical single aperture. The teflon separator also has a vacuum output individually at the bottom of it. The vacuum output is also shown as a red vacuum pipe in Figure 5.16. The blue plastic pipes are used to isolate the bolts and nuts in order to prevent any short circuits between the first single aperture and the conical single aperture.

(a) Profile

(b) Teflon Separator Side

(c) Vacuum Gradient Side
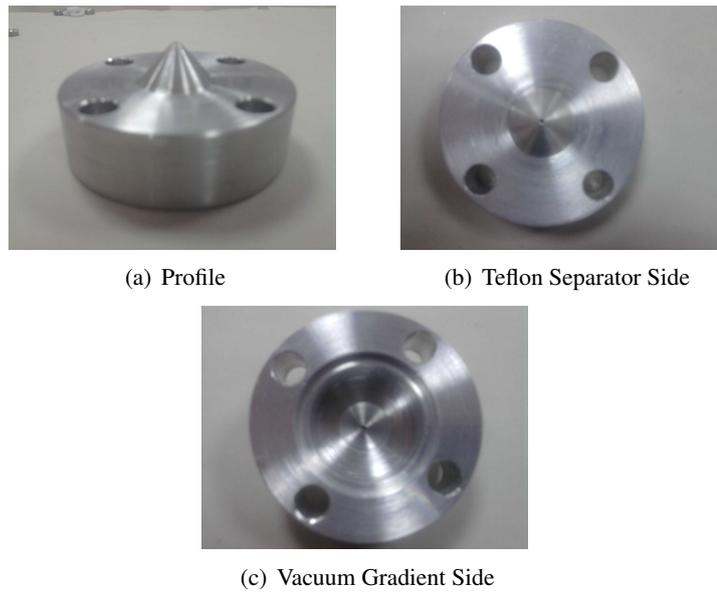
Figure 5.15: The Conical Single Aperture

Figure 5.16: The Teflon Separator

The vacuum gradient part is shown in Figure 5.17 with its connection disks and a vacuum pump connector. The left side of the vacuum gradient part is connected to the conical single

aperture with an O-ring and a connection disk. The right side of it is connected to the Faraday cup in order to measure the ion beams. In addition to them, the connection of the underside joins with the high vacuum pump in order to produce very low pressure gradient. While the pressure, inside the teflon separator, is in between 10^{-1} and 10^{-2} mbars, the inside of the vacuum gradient part can be at the pressure of the order of 10^{-3} mbars.

Before starting the experiment, the whole system is cleaned in order to use hydrogen gas in the experiment. After that, the whole system pressure is brought to a desired pressure and then the vacuum gradient side is brought to lower pressures to elongate the mean free path of the ions. So they can travel more distance without collisions. If the inside of the teflon separator is held at a constant pressure, the vacuum gradient will be sustained through the whole system, from the gas inlet to the target.

Figure 5.17: The Vacuum Gradient Part

The vacuum gradient part plays a very crucial role in this experiment. If the pressure is not low enough inside the vacuum gradient part, which takes place in between the conical single aperture and the Faraday cup, a DC discharge can be induced between the conical single aperture electrode and the metal flange of the Faraday cup. It is important to prevent this

DC discharge for measuring the accurate data of ion current, produced by the microwave induced plasma and its corresponding extraction unit. The pressure, inbetween the extraction electrodes, changes from the order of 10^{-1} mbars to the order of 10^{-2} mbars (from the order of 10^{-2} torr to the order of 10^{-3} torr). The estimated Paschen curve of the hydrogen gas, in Figure 2.4, is used for determining the critical value of the DC breakdown. If the highest pressure value, 10^{-2} torr, is taken into account, the value of pd becomes 5×10^{-3} torr-cm for the minimum separation of 5 mm, between the extraction electrodes. If the corresponding breakdown voltage is found from Figure 2.4, it is seen that the value of the breakdown voltage exceeds the value of 10kV. In the designed system, merely 3kV is applied between the extraction electrode and the Faraday cup. Therefore, the occurance of the DC discharge plasma is prevented.

5.3   MEASUREMENTS OF ION CURRENT

While measuring the ion current, a Faraday cup is used. A Faraday cup is a device which measures the current of charged particles. The basic theory of the Faraday cup is that a cup shaped metal faces the incoming charged particles. The impinging charged particles charge up the Faraday cup and it gains a net charge. The Faraday cup discharges this small amount of the ion accumulation by grounding. If this small amount of current is measured by an electrometer then the current of the ions, entering the Faraday cup, is determined. The number of ions per second, entering the Faraday cup, N is given by,

$$N = It/e \quad ,$$
(5.6)

where I is the measured current (in Amperes), t is the time interval(in seconds) when the measurement is done, and e is the electronic charge (in Coloumbs). The above equation can be assumed as a good approximation for the ions, having the ionization state of one.
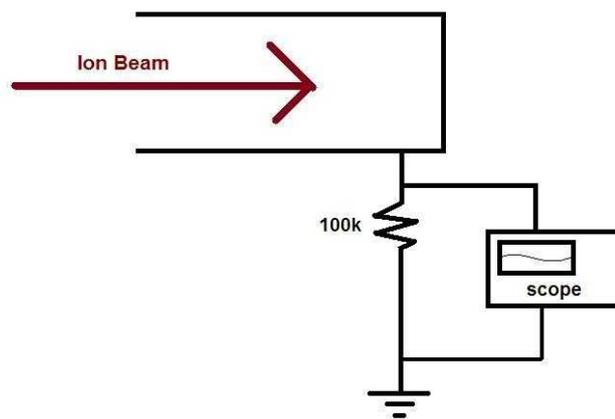

Figure 5.18: The Faraday Cup Scheme

If a resistor is connected between the Faraday cup and the ground in series, the voltage drop can be measured over this resistor and the amount of current can be calculated in order to neutralize the incoming beam, impinging into the Faraday cup. An electrometer can also be connected in series instead of the resistor. The Diagram is depicted in Figure 5.18. Figure 5.18 also shows the principal circuit diagram of the measurement unit of the microwave ion source. In this system, there is a resistor with a resistance of 100 $k\Omega$ in series and the voltage is read on this resistor by a scope.

For the measurements of this microwave ion source, the Kimball Physics model FC-73A Faraday cup is used. The Faraday cup consists of two parts as it is shown in figures 5.19 and 5.20. In Figure 5.19, the part, numbered as (1), is the converter and connection part of the Faraday cup, joining the vacuum gradient part. And the second part, numbered as (2), is the head of the Faraday cup. At the most-right of the Faraday cup, there are three BNC connections which are used for different purposes. The current reading BNC connection of the Faraday cup is numbered as (3). Both the converter-connection part and the head of the Faraday cup is made of stainless steel. A copper O-ring is placed between the part (1) and the part (2) while joining them together.
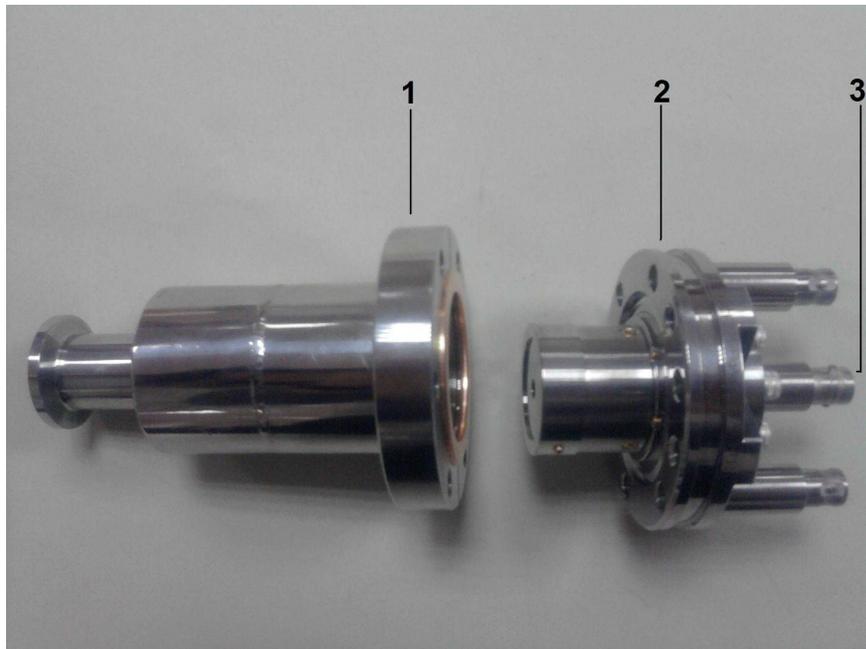
Figure 5.19: The Faraday Cup (side view)

The profiles of the parts are shown in Figure 5.20. The head of the Faraday cup has an aperture with the diameter of 5 mm. The incoming ion beam impinges on this aperture. The area of this aperture is $0.196cm^2$.
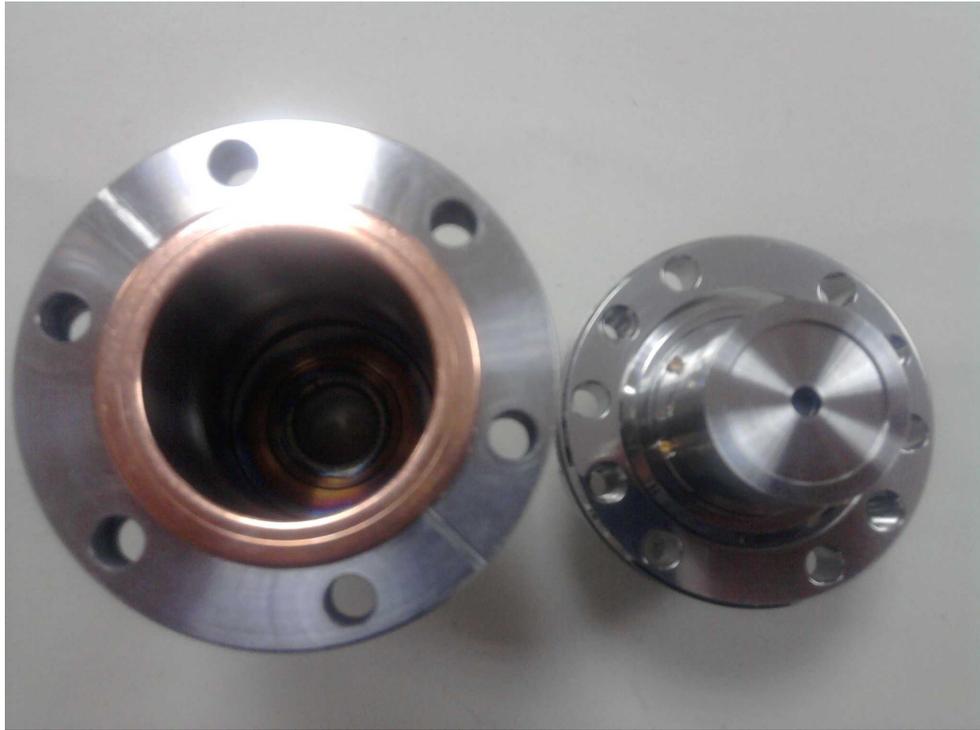
Figure 5.20: The Faraday Cup (inside view)

In this work, the microwave induced hydrogen plasma was generated at the pressure of 1.5 mbars and the extraction voltage, V_{ext} was applied to the first single aperture at a voltage of $3kV$. Moreover, the conical single aperture and the frame of the Faraday cup were grounded. The vacuum gradient part was kept at a pressure of order of 10^{-3}mbars. At this plasma pressure and extraction voltage, V_{ext}, the impinging ion current was measured as $25\mu A$, passing through the aperture of the Faraday cup with an area of $0.196cm^2$. The total current, passing through per centimeter square was calculated as $125\mu A$.

The trajectory of the generated ions were simulated with the actual dimensions of the system. The simulations were done with the computer programme, known as SIMION Version 8.0.

The simulation of the ion trajectories were made for 20 protons, in the vicinity of the first single aperture without any thermal energies. The protons were accelerated by $3kV$. The aperture of the Faraday cup was located at the most-right end of the simulation screen. For low densities, the focusing of the particles can be achieved by the geometry of the extraction apertures and the extraction electrodes. The side view of the simulation of the system is shown in Figure 5.21.
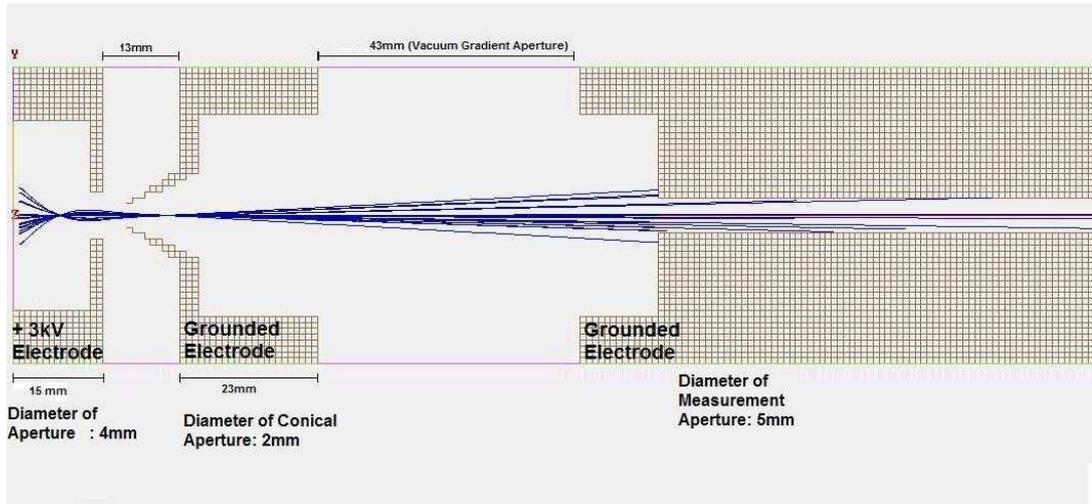
Figure 5.21: The side view of the simulation of the system

In Figure 5.22, the voltage topography of the simulation can be seen; in addition to this, the motion of the particles can be easly perceived through the voltage downstream.
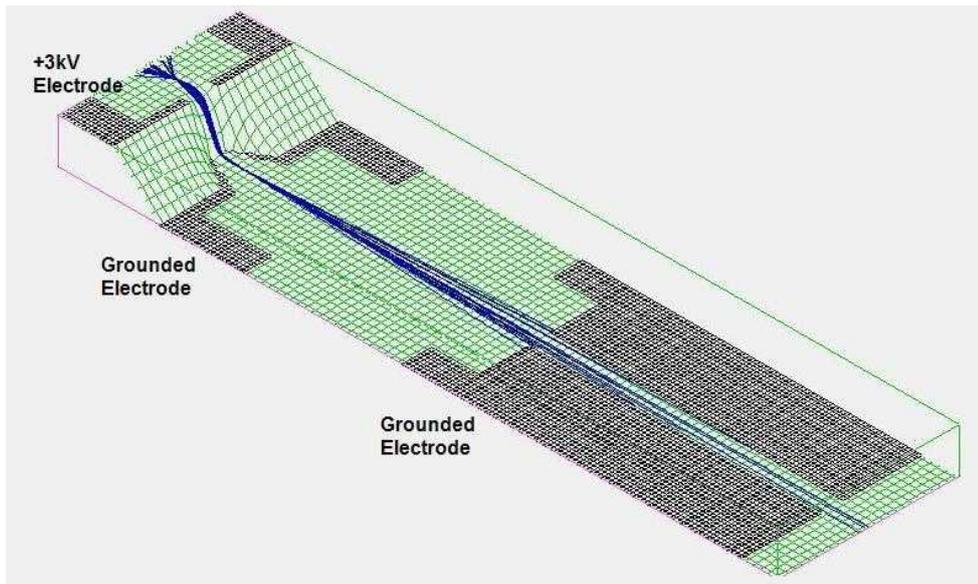

Figure 5.22: The voltage topography of the simulated system

CHAPTER 6

DISCUSSION AND CONCLUSION

In this thesis, the microwave induced plasma ion source was investigated in detail. In order to achieve this, the ion production via plasma by using a microwave radiation and ion extraction systems were discussed. Moreover, microwave source design and plasma induction systems were studied. In order to obtain and to have the knowledge of the plasma parameters, the double Langmuir probe techniques were considered and applied. The vacuum gradient was constituted and used in order to increase the mean free path of the extracted ions.

In order to prevent the electrical breakdown between the extraction electrodes the estimated Paschen curve for the hydrogen gas, in Figure 2.4, was drawn and used to verify the clear extraction without any breakdown. The estimated value of the breakdown voltage is more than 10 kV from the estimated graph in Figure 2.4, for the minimum separation of 5 mm and it is also consistent with Equation 6.1 [1].

$$d \geq 1.41 \times 10^{-2} V \qquad (6.1)$$

where d is the separation distance of the extraction electrodes, in units of milimeter (mm) and V is the extraction voltage, in units of kilovolt (kV) between the electrodes. For this designed system, the relation was found for the minimum separation gap, $d = 5mm$, and the extraction voltage, $V = 3kV$, as

$$5mm \geq 1.41 \times 10^{-2}(3kV)$$

$$5mm \geq 7.3 \times 10^{-2}mm$$

Our designed and constructed system worked as it was expected. However, some errors occured while taking the data at the midpoint of the waveguide. Before discussing the main errors, the known errors should be made clear.

There was an anomaly for the plasma density at the midpoint of the waveguide. The electron density was decreasing, when the probe tips were drawn out of the waveguide as it was expected. However, the data measurements at the midpoint were not accurate. The calculated value of the density is in the order of $10^8 cm^{-3}$ and it is much smaller than the values, which were calculated for the dispersion zones. There is a contradiction and, to analyse this situation, a good filtration and an isolation should be done for the double Langmuir probe. When the probe tips were immersed into the waveguide area, the microwave radiation could cause sparks or generate plasma regions in between the pyrex probe tube through which the tungsten probe wires crossing. In addition to these, there could be one more reason. The density of the particles decreases in a great deal while they spread towards the waveguide borders. And also the TEM mode of the microwave sustains this distrubution while it decreases its field strength. Moreover, the one of the nodes of the standing wave was close to the pyrex plasma tube, the tips were not located accurately. If the tips had been moved a little bit out of its determined location, the data would not been measured accurately. The dislocating the tips is the other reason of not measuring the maximum values of the plasma parameters at the midpoint of the waveguide where the plasma parameters reach the maximum values as they are expected to be. When the probe tips were drawn away from the waveguide borders, where the dispersion began, the electron density decreased as it was expected.

As a result, the microwave ion source system was designed and constructed by generating the hydrogen plasma. The plasma was generated by using the microwave source with the frequency of 2.45 GHz and the power of 700 Watt. The generated microwave was pulsing with the frequency of 50 Hz. The plasma parameters were taken by the double Langmuir probe and the ion current was measured by the Faraday cup. The designed and constructed microwave system generated the hydrogen plasma with $\sim 10^{10} cm^{-3}$ electron density (n_e) and $\sim 2eV$ electron temperature (T_e) in the pyrex chamber (tube) at the pressure of 1.5 mbar in the region, out of the microwave-guide, where the plasma dispersed.

By refering Equation 6.2, there is an upper limit for the electron density, n_e, of the plasma and it is about $n_e = 6.66 \times 10^{10} cm^{-3}$. For the calulated values from the I-V curves, mentioned

above and also in 'Chapter 5', the maximum value of the electron density was found as $2 \times 10^{10} cm^{-3}$ at the outside borders of the waveguide, so the density values verify the theoretical inequality, mentioned below. And the density also decreases rapidly in few milimeters from $10^{10} cm^{-3}$ to $10^9 cm^{-3}$ order.

$$n_e(= n_i) \leq 1.11 \times 10^{10} f^2 \tag{6.2}$$

$$2 \times 10^{10} cm^{-3} \leq 6.66 \times 10^{10} cm^{-3}$$

For the ion extraction part, an ion current was generated by the designed system and the measurements were done by the Faraday cup. The ion current was measured as $125\ \mu A/cm^2$ at a distance of approximately 125 mm away from the second extraction electrode by applying the extraction voltage of 3 kV to the first single aperture electrode and grounding the conical single aperture and the frame of the Faraday cup.

In Figure 6.1 [11], three ion extraction processes are given with different plasma densities. The densities increase as $n_1 \leq n_2 \leq n_3$ and the extraction voltage is held constant. If the plasma density is too low then the plasma border (plasma meniscus) forms a concave shape with the extraction voltage. With increasing density this concave shape turns out to be a convex shape. After the second electrode, the ions travel a distance, they repel each other and there occurs a divergence because the electric field is created by the ions. As a result, the ions repels each other due to this electric field.
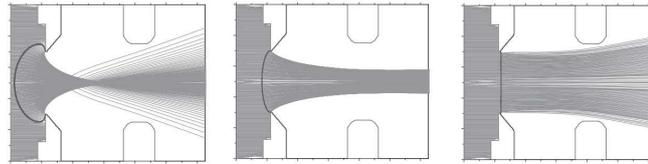

Figure 6.1: AXCEL-INP simulation for a diode system with three plasma density and the same voltage drop. From left to right:$n_1 \leq n_2 \leq n_3$ [11]

In figures 5.21 and 5.22, the convex shape is seen clearly before they leave the second electrode and the divergence is formed after the second electrode. This divergence can be controlled by a triode extraction system and by an Einzel lens. If a collimation is done by this way, the beam quality can be increased. The Einzel lens system should be added to the beam line to provide the collimation through the beam line.

For the designed system, the parameters of the ions, such as the perveance, $\mathcal{P}$, so the ion current, I_i should be compared with the value of the maximum perveance, $\mathcal{P}_{max}$, so the maximum extractable ion current, I_{imax}. The values of the parameters are calculated by

$$\mathcal{P}_{max} = \frac{\pi\varepsilon_0}{9}\sqrt{\frac{2(1.6\times10^{-19}C)}{(1.67\times10^{-27}kg)}}\left(\frac{1mm}{13mm}\right)^2 \qquad (6.3)$$
$$= 2.53\times10^{-10}(A/V^{3/2})$$

If the maximum perveance, $\mathcal{P}_{max}$, is multiplied by the extraction voltage, V_0, of 3000 volts, the maximaum ion current, in the vicinity of the conical single aperture, is found:

$$I_{imax} = 2.53\times10^{-10}\times3000^{3/2} \qquad (6.4)$$
$$= 4.16\times10^{-5}(A) = 41.6(\mu A)$$

The measured value of the ion current is $25\mu A$. If the theoretical and measured values are compared, the ion efficiency, η_{a-a}, between the conical single aperture and the aperture of the Faraday cup is found as:

$$\eta_{a-a} = \frac{25}{41.6} \qquad (6.5)$$
$$= 0.60$$

The percentage of the ion efficiency is 60%. Also it can be seen from Figure 5.21 that 12 of 20 particles can reach into the middle of the grounded electrode where the measurements were taken. The measured value, above, is consistent with the value, which is found from Figure 5.21. These values, for the ion current readings, were done without applying any Einzel lensing or any collimation process for the extracted ion beam.

For the further research, the relations between the microwave plasma parameters and the perveance parameter can be invesitaged by changing the extraction voltage, plasma pressure. In addition to them, the design of the extraction apertures can be changed and effects on the perveance can be investigated further.

REFERENCES

[1] B.H. Wolf. *Handbook of Ion Sources*. CRC Press, Inc., Boca Raton ;New York; London; Tokyo, 1995.

[2] J.R. Roth. *Industrial Plasma Engineering*, volume 1. Institute Of Physics Publishing, Bristol, 2001.

[3] M. Konuma. *Plasma Techniques for Film Deposition*. Alpha Science International, Harrow, U.K., 2005.

[4] F.F. Chen. *Introduction to Plasma Physics and Controlled Fusion*, volume 1. Plenum Press, New York, 1984.

[5] A. Grill. *Cold Plasma in Metarials Fabrication: from Fundamentals to Applications*. Institute of Electrical and Electronics Engineers Press, Inc., Piscataway, NJ, 1994.

[6] A. Ganguli and R.D. Tarey. Unserstanding plasma sources. *Current Science*, 83(3):279–290, August 2002.

[7] A. Fridman and L.A. Kennedy. *Plasma Physics and Engineering*. Taylor and Francis, New York, 2004.

[8] M.A. Lieberman and A.J. Lichtenberg. *Principles of Plasma Discharges and Metarials Processing*, page 547. Willey, Hoboken, New Jersey, 2 edition, 2005.

[9] M.A. Lieberman and A.J. Lichtenberg. *Principles of Plasma Discharges and Metarials Processing*, page 460. Willey, New York, 1 edition, 1994.

[10] D.M. Pozar. *Microwave Engineering*, pages 104–141. Wiley, New York, 2 edition, 1998.

[11] I.G. Brown. *The Physics and Technology of Ion Sources*. Willey-VCH, Weinheim, 2 edition, 2004.

[12] A. Fridman and L.A. Kennedy. *Handbook of Plasma Processing Technology : Fundamentals, Etching, Deposition, and Surface Interactions*. Noyes Publications, Park Ridge, N.J., U.S.A., 1990.

[13] R.H. Huddlesyone and L.L. Stanley. *Plasma Diagnostic Techniques*. Academic Press, New York, 1965.

[14] Yang Z. Xiao K. Jin, D. and J. Dai. Diagnosis of hydrogen plasma in a miniature penning ion source by double probes. *Plasma Science and Technology*, 11(1):48–51, February 2009.